Nanoscale

Accepted Manuscript

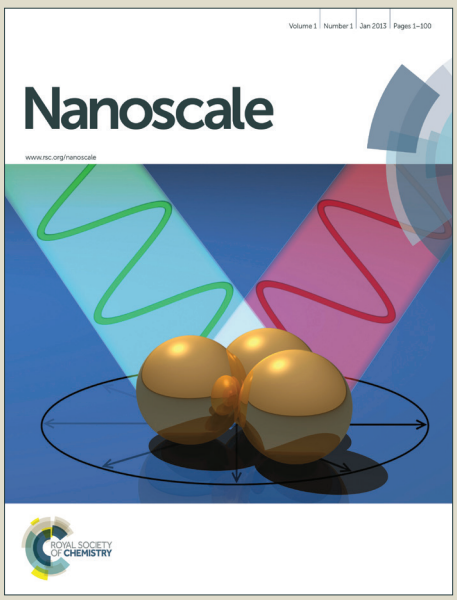

ROYAL SOCIETY OF CHEMISTRY

www.rsc.org/nanoscale

Journal Name

RSCPublishing

ARTICLE

Nanoarchitectonics of biomolecular assemblies for functional applications

Cite this: DOI: 10.1039/x0xx00000x

M. B. Avinash,[a] and T. Govindaraju*[a]

Received 00th January 2012,
Accepted 00th January 2012

DOI: 10.1039/x0xx00000x

www.rsc.org/

The stringent processes of natural selection and evolution have enabled extraordinary structure-function properties of biomolecules. Specifically, the archetypal designs of biomolecules such as amino acids, nucleobases, carbohydrates and lipids amongst others encode unparalleled information, selectivity and specificity. The integration of biomolecules either with functional molecules or with an embodied functionality ensures an eclectic approach for novel and advanced nanotechnological applications ranging from electronics to biomedicine, besides bright prospects in systems chemistry and synthetic biology. Given this intriguing scenario, our Feature Article intends to shed light on the emerging field of functional biomolecular engineering.

1 Introduction

Biomolecules are the organic molecules produced within a living cell.[1] They may be small or macro-sized, formed as a product of biochemical reactions and render specific functions to biological processes.[2] These biomolecules are the outcome of nearly four billion years of natural selection and evolution.[3] Unsurprisingly, the biological systems comprising a plethora of biomolecules exhibit remarkable structure-property correlations, selectivity, specificity and complexity.[4] Due to these intriguing attributes, the current research efforts are ventured on the exploitation of these biomolecules to generate various functions and also to better understand the complex biochemical processes.[5-12] In this context, we conceptualized the process of custom-designing and engineering the molecules of biological origin as biomolecular architectonics (Fig. 1).

Herein, we restrained ourselves to the architectonics of the key biomolecules, namely, amino acids, nucleobases, carbohydrates and lipids. As these biomolecules are the basic building blocks that can create highly diverse organisms through various permutations and combinations, the very process of engineering their assemblies *via* a bottom-up approach ensures innumerable opportunities for various nanotechnological applications.[13-19] At the same time, it is important to note that the attainment of pre-programmable

M. B. Avinash obtained his Integrated MSc (Hons.) in Applied Chemistry from Kuvempu University, Karnataka, India in 2008.

He was selected for the Project Oriented Chemical Education (POCE, 2004–2006) and Summer Research Fellowship (SRF, 2007) programs of JNCASR. After his graduation he worked as a Research & Development Personnel for Defence Research & Development Organization (DRDO) project at JNCASR. Following which he pursued his PhD under the supervision of Prof. T. Govindaraju. Currently, he is working as a Research Associate for a DRDO project at JNCASR. His research interests include Nature-inspired molecular engineering of biomolecules and its derivatives to develop advanced functional molecular materials.

T. Govindaraju is an Associate Professor at New Chemistry Unit, JNCASR, Bangalore, India. He received his MSc in Chemistry (2000) from Bangalore University and PhD in Chemistry (2005) from National Chemical Laboratory and University of Pune, India. He carried out postdoctoral work (2005–2006) at the University of Wisconsin-Madison, USA. He received the Alexander von Humboldt postdoctoral fellowship and worked (2006–2008) in the Max Planck Institute of Molecular Physiology, Dortmund, Germany. His research interests are at the interface of chemistry, biology and materials, including organic synthesis, peptide chemistry, neurodegenerative diseases, nucleic acid chemistry, molecular probes and nanobiotechnology.

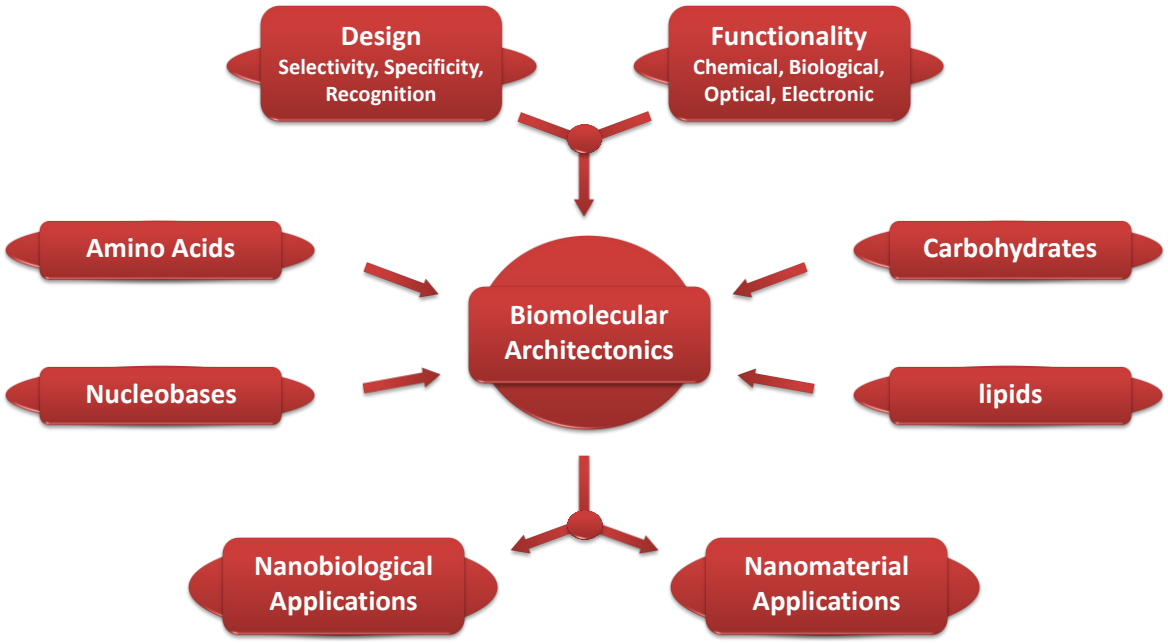

Fig. 1 Biomolecular architectonics for nanobiological and nanomaterial applications.

assemblies and functions, is a challenging task due to the delicate and complex interplay of several noncovalent interactions of biomolecules.[20-23] In addition, as different biomolecules possess distinct chemical functionalities, the design principles embraced for their controlled assemblies are also unique. Thus, it is imperative that this field of biomolecular engineering is embarking on a cutting edge research methodology so that its full potential could be realized in the near future.

The article is structured into four sections titled as *architectonics of functional amino acids*, *architectonics of functional nucleobases*, *architectonics of functional carbohydrates* and *architectonics of functional lipids*. Each of these four sections is further divided into two subcategories namely *nanobiological applications* and *nanomaterial applications*. Herein, we mainly focus on the design strategies of functional biomolecules and its role in attaining the preprogrammed property for appropriate applications. In the *nanobiological applications* subcategory, elegant utilization of designer biomolecules for biomineralization, cell growth, cell differentiation, tissue repair, bone regeneration, sequence-specific DNA intercalation, antitumour activity, antimicrobial activity, diagnostics, therapeutics and others have been presented. On the other hand, the tailored assemblies of functional biomolecules for light harvesting, energy transfer, charge transfer, photonics, piezoelectricity, ferroelectricity, pyroelectricity, catalysis and sensing have been discussed under *nanomaterial applications* subcategory. Finally, perspectives for further progress have been delineated in the *future outlook* section. It should be noted that this Feature Article is an account of selectively chosen reports in an effort to provide an enticing flavour of this emerging field and not intended to be an exhaustive resource of literature.

2. Architectonics of functional amino acids

Amino acids are biomolecules consisting of amine and carboxylic acid functionalities, with distinct side-chain groups. Covalent linkages of amino acid residues *via* CO-NH peptide bonds result in the formation of polypeptides, popularly known as proteins. There are over twenty different α-amino acids depending on the nature of the side-chain, which in turn impart hydrophobic, hydrophilic, cationic or anionic characters to the molecules. Each of these biologically important amino acids is denoted by three or single letter abbreviations as shown in Fig. 2. Depending on the sequence of amino acids, the so formed protein attains a unique three-dimensional structure and thereby offers specific functions *viz*. that of catalyst, regulator, replicator and/or transporter besides others.[24] In an effort to emulate the properties of such functional amino acids, considerable efforts have been made in the recent past and the details of which formulate the contents of this section.

2.1 Nanobiological applications

Nearly two decades ago, an ingeniously designed amino acid derivative was reported to create a well-defined protein-like molecular architecture via a minimalistic approach.[25] Besides similar efforts[26,27], amino acid based nanostructured fibrous scaffold akin to extracellular matrix was developed.[28] This latter designer molecule was a peptide amphiphile **1**, which can be dissected into five key structural features (Fig. 3). Region-I comprised of a long alkyl hydrophobic tail, while regions-II, -III, -IV and -V comprised of specific sequences of amino acids. The cysteine residues of region-II, when oxidized facilitate the formation of disulfide bonds to polymerize the self-assembled

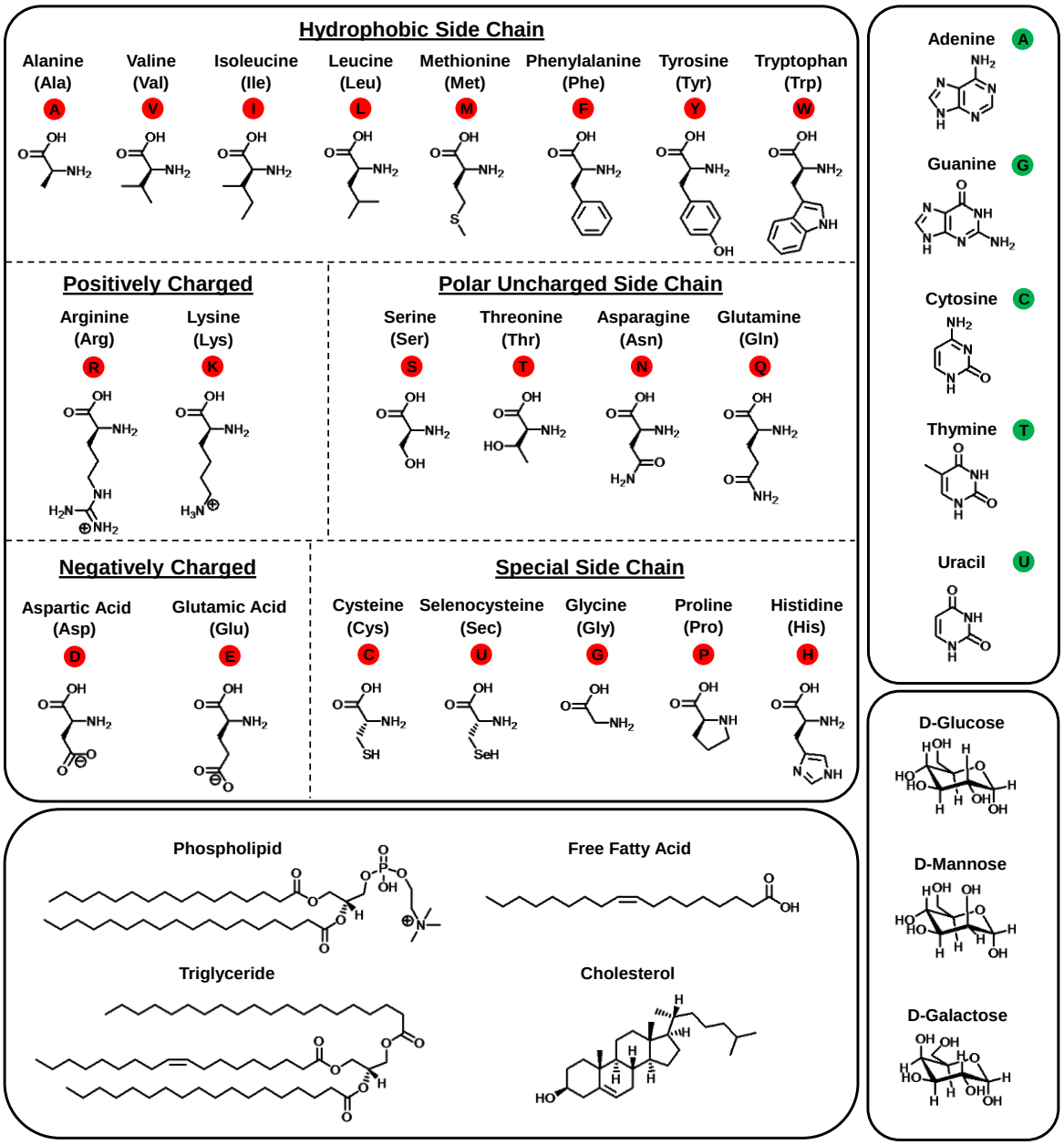

Fig. 2 Molecular structures of amino acids, nucleobases, carbohydrates and lipids along with their commonly used abbreviations.

structure. The glycine residues of region-III act as a flexible linker, and the phosphorylated serine residue of region-IV directs the mineralization of hydroxyapatite *via* strong interaction with calcium ions. The region-V comprises of arginine-glycine-aspartic acid residues, which acts as a cell-adhesion ligand. The conical shape of the peptide amphiphile dictates their self-assembly into cylindrical nanofibres (Fig. 3a). Further, these nanofibres were reported to direct the mineralization of hydroxyapatite into a composite material, wherein the crystallographic *c* axis of hydroxyapatite was aligned along the long axis of the fibres, which is similar to that of collagen fibres and hydroxyapaptite crystals in bone. Additional studies went on to demonstrate that only one-dimensional (1D) cylindrical nanostructures direct the growth of oriented hydroxyapatite crystals, whereas flat nanostructures result in random orientations of the crystals.[29] This biomimetic strategy was also tested in a rat femoral critical-size defect by placing pre-assembled nanofibre gels in a 5 mm gap, which showed significantly higher bone formation relative to controls lacking phosphorylated residues.[30] In another study, histidine-rich peptide amphiphile fibres were employed as templates for the growth of magnetite nanocrystals, which are similar to that found in bacterial magnetosomes.[31] However, the crystallographic alignment of the synthetically obtained crystals were not the same as that of the magnetotactic bacteria, which enables it to find appropriate oxygen levels in the ocean using the geomagnetic field.

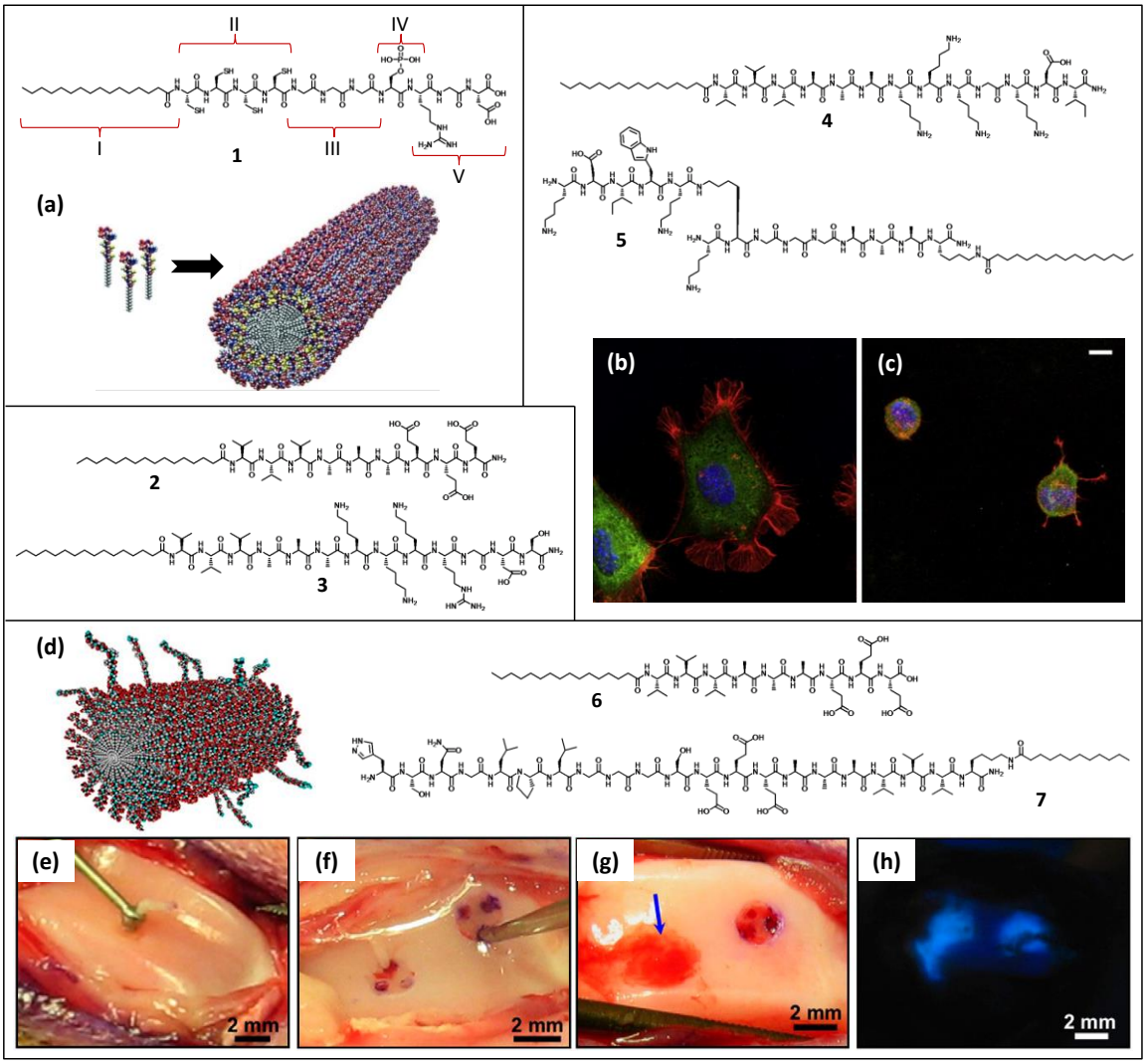

Fig. 3 Molecular structures of amino acid derivatives. (a) Schematic showing the self-assembly of **1** into a cylindrical nanofiber. Reproduced with permission of American Association for the Advancement of Science from ref. 28. (b) and (c) Fluorescent micrographs show the 3T3 fibroblasts morphology on stiff (**4**) and soft (**5**) amino acid derivatives, respectively. They were plated and stained with phalloidin (red), anti-vinculin antibody (green) and DAPI (blue). Reproduced with permission of Elsevier from ref. 38. (d) Schematic shows the co-assembled nanofibre of TGF-binding peptide and the filler peptide amphiphile with the binding epitopes exposed on their surface. (e) Full thickness articular cartilage defects in rabbit trochlea created by microcurette. (f) Microfracture holes through the subchondral bone to induce bleeding into the defect by using a microawl. (g) Peptide amphiphile gel in defect after injection (arrow) and (h) the containment of pyrene-labelled gel within the defects after injection. Reproduced with permission of National Academy of Science (USA) from ref. 40.

Recently, cell-based therapies have drawn considerable clinical interest for ischemic tissue repair in cardiovascular diseases.[32] However, poor cell viability and minimal retention following application were reported to limit the regenerative potential of these therapies. To circumvent these issues, the bioactive peptide amphiphile nanofibres displaying the fibronectin-derived RGDS, cell adhesion epitope was developed as a scaffold for therapeutic delivery of bone marrow-derived stem and progenitor cells.[33] A binary peptide amphiphile system consisting of 10 wt% RGDS-containing molecules (**2**) and 90 wt% negatively charged diluent molecules (**3**) was found to promote optimal cell adhesion, besides enhancing cell viability and proliferation. Peptide amphiphilic design strategy was also employed to promote angiogenesis by mimicking the activity of VEGF (Vascular Endothelial Growth Factor), which is one of the most potent angiogenic signalling proteins.[34] The designer molecule was reported to comprise of a peptide sequence that mimics VEGF, i.e., KLTWQELYQLKYKGI-NH_2 with its N-terminus linked to a K_3G sequence to facilitate solubility. The V_2A_2 β-domain was followed by a C_{16} alkyl chain to promote the self-assembly into cylindrical nanostructures. These nanofibres induced phosphorylation of VEGF receptors and promoted proangiogenic behaviour in endothelial cells as well as in a hind-limb ischemia model of cardiovascular disease. In addition, a study reported the promotion of rapid angiogenesis by utilizing heparin-binding growth factors involved in signalling angiogenesis.[35]

Remarkably, when the laminin pentapeptide epitope (IKVAV) was incorporated in the peptide amphiphile design,

very rapid differentiation of cells into neurons was observed while discouraging the development of astrocytes.[36] This was attributed to the 1000-fold amplified presentation of bioactive epitopes to cells in the case of nanofibres. Moreover, when these nanofibres were employed in the *in vivo* treatment of spinal cord injury, they effectively reduced astrogliosis, reduced cell death and increased the number of oligodendroglia at the site of injury.[37] It is to be noted that neuronal differentiation and maturation are influenced by the mechanical properties of the extracellular matrix.[38] In this regard, the extracellular matrix mimicking self-assembled peptide nanofibres with tailored rigidity was investigated to probe the relationship between matrix stiffness and morphological development of hippocampal neurons. The rigidity of the peptide nanofibres was modulated based on the two simple hypotheses: 1) the amino acids with a strong propensity to form β-sheet secondary structures enable increased stiffness, and 2) increased bulkiness of the molecule affects their packing density. In addition, a bioactive peptide sequence KDI, was incorporated, which is known to promote neurite outgrowth and axon guidance. The so designed stiff (**4**) and soft (**5**) peptide amphiphiles exhibited characteristic circular dichroism signals corresponding to β-sheet and random coil structures. Moreover, the gels of **4** were found to have three times higher storage modulus than that of **5**, although the stiffness of the individual fibres could be different. It was observed that the development of neuronal polarity was accelerated on soft nanofibre substrates and their weaker adhesion facilitated easier retraction, thus enhancing the frequency of extension-retraction events (Fig. 3b, c). The higher neurite motility was thought to enhance the probability of one neurite to reach a critical length relative to others and thereby initiate the developmental sequence of axon differentiation.

A self-assembling peptide hydrogel of $(KLD)_{12}$ was shown to act as a scaffold for encapsulation of chondrocytes.[39] The alternating hydrophobic and hydrophilic residues on the backbone of $(KLD)_{12}$ promoted β-sheet formation and facilitated self-assembly through intermolecular interactions. During four weeks of *in vitro* culture, these chondrocytes developed a cartilage-like extracellular matrix rich in proteogylcans and type-II collagen, indicative of a stable chondrocyte phenotype. Moreover, the time-dependent enhancement in the material stiffness indicated the deposition of mechanically functional neo-tissue. In a novel co-assembly design strategy, high density of epitopes binding to transforming growth factor β-1 (TGFβ-1) were developed to engender cartilage regeneration.[40] Non-bioactive peptides (**6**) of smaller molecular dimensions were co-assembled with TGFβ-1 binding peptides (**7**), so that the binding epitope could adequately capture and display the growth factor for signalling (Fig. 3d). Further studies showed that these materials promote regeneration of articular cartilage in a full thickness chondral defect, treated with microfracture in a rabbit model with or without the addition of exogenous growth factor (Fig. 3e-h).

A peptide amphiphile containing the peptide sequence $V_3A_3E_3(CO_2H)$ and an *N*-terminus C_{16} alkyl chain resulted in nanofibrillar assemblies similar to those described above.[41] Interestingly, when the aqueous solution of this peptide was annealed at 80 ^oC, the solution viscosity increased threefold, whereas in the presence of calcium chloride, gels were produced with at least fourfold higher stiffness. By drawing the heated aqueous peptide solution into salty (aqueous calcium chloride) medium, noodle-like strings of arbitrary length as well as large birefringent domains were obtained due to aligned peptide nanofibres (Fig. 4a). By following the above-mentioned annealing procedure with human mesenchymal stem cells and the peptide solution, noodle-shaped strings with encapsulated stem cells were obtained (Fig. 4b, c). Further utilization of this 'cellular wire' concept to serve as a bridge for spatial direction of cells for function or migration from one site to another was demonstrated by employing HL-1 cardiomyocytes, a cell-line with spontaneous electrical activity that requires extensive cell-cell contacts to propagate signals. In a recent report, the aligned peptide nanofibres scaffold was specifically designed to support neural cell growth and function.[42] The growth of neurites from neurons encapsulated in the scaffold was enhanced by the presentation of IKVAV or RGDS epitopes while the alignment guided these neurites along the direction of nanofibres (Fig. 4d).

Inspired by the promising utilization of oligopeptide-based hydrogels as scaffold material for cell cultures and tissue engineering, relatively smaller functional dipeptides were also employed as scaffolds for three dimensional (3D) cell cultures.[43] As per another report, a simple amino acid derivative that was internalized into the cell could also regulate cell death by enzymatic control.[44] Herein, the functional molecule consists of three distinct motifs: 1) phenylalanine-based dipeptide to engender hydrogen bonds; 2) a napthyl group to facilitate hydrophobic force-induced self-assembly in an aqueous environment, and 3) a butyric diacid-based ester that could be cleaved by an enzymatic trigger. These peptides were internalized by HeLa cells while the endogenous esterases cleaved the butyric diacid-based ester to aid nanofibrillation and cell death. Therefore, by incorporating suitable substrates susceptible to different enzymes, highly sophisticated controls could be envisioned. Another approach was the intracellular delivery of cytotoxic peptides to induce cancer cell death.[45] This was achieved by employing a cationic α-helical $(KLAKLAK)_2$ peptide (that is known to induce cancer cell death by membrane disruption) into an amphiphilic design so as to obtain bioactive cylindrical nanofibres.

It was recently reported that cell-penetrating peptides (**8**) that can encapsulate hydrophobic drug molecules inside the peptide nanostructures have also been developed (Fig. 4e).[46] The peptide comprised of three functional blocks *viz.* a Tat block (GRKKRRQRRRPPQ), a flexible linker block (GSGG) and a β-sheet assembly block (FKFEFKFEFKFE). The Tat block is a segment of human immunodeficiency virus type-1 (HIV-1) Tat protein, which can efficiently cross the cytoplasmic membrane and the nucleus pore complex barriers. In a similar approach, peptide amphiphiles were used to encapsulate the hydrophobic drug camptothecin in its

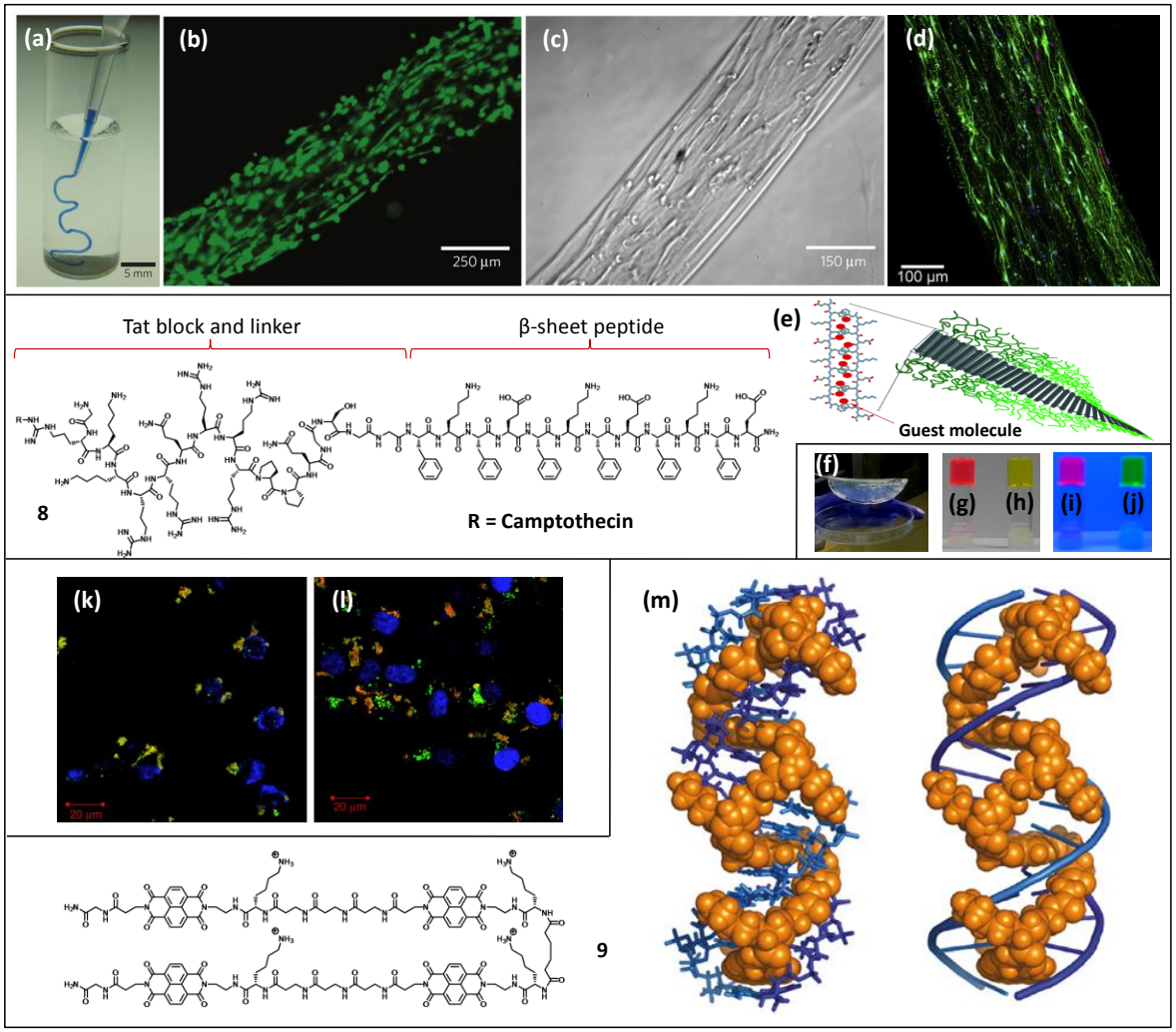

Fig. 4 Molecular structures of amino acid derivatives. (a) Injection of peptide amphiphile colored with trypan blue into phosphate-buffered saline after heat treatment. Alignment of (b) calcein-labelled cells cultured in string, (c) encapsulated hMSCs along the string axis and (d) Hippocampal neurons [stained for β-III-tubulin (green), GFAP (red) and DAPI (blue)]. Reproduced with permission of (a-c) Nature Publishing Group from ref. 41 and (d) Elsevier from ref. 42. (e) Schematic showing the encapsulation of hydrophobic guest molecules within the peptides. Reproduced with permission of Wiley-VCH from ref. 46. (f) Organogel formed from a cyclic dipeptide (CDP) derivative made up of glycine and L-lysine. Rhodamine B and curcumin entraped organogel of CDP derivative visualized under visible light [(g) and (h)] and UV light [(i) and (j)] respectively. Reproduced with permission of Royal Society of Chemistry from ref. 48. (k) and (l) Confocal images of HepG2 cells treated with FITC-loaded peptide micelle/rhodamine-labelled DNA complexes formed at N/P (defined as the ratio of peptide to DNA) 18 after 4 h and 24 h, respectively. Reproduced with permission of Elsevier from ref. 49. (m) A model illustrate the complexation of tetra-intercalator, **9** with 3-d(GATAAGTACTTATC)$_2$. Reproduced with permission of Nature Publishing Group from ref. 50.

biologically active lactone form for chemotherapeutic applications.[47] Analogously, we have shown that cyclic dipeptide (CDP) based low-molecular weight derivatives made up of glycine and L-lysine exhibit organogelation properties (Fig. 4f).[48] Additionally we have also shown that hydrophobic moieties like rhodamine B and drugs like curcumin could be incorporated within these gels, which finds utilization in various biological applications (Fig. 4g-j). In another report, an oligopeptide [Ac-$(AF)_6$-H_5-K_{15}-NH_2] was found to self-assemble into cationic core-shell nanostructures (i.e., micelles) with a critical micellar concentration of 0.042 mg/mL, average size of ~100 nm and a zeta potential of about 23 mV.[49] These peptide micelles were investigated for their utilization as nanocarriers for co-delivery of drug and gene. Further studies showed that the simultaneous delivery of both p53 gene and doxorubicin *via* these nanocarriers resulted in increased expression of p53 mRNA as well as enhancement in end point cytotoxicity towards HepG2 cells (Fig. 4k, l). Interestingly, molecules that can bind DNA are considered as interesting prospects to modulate transcription, repair and replication both *in vitro* and *in vivo*. Moreover, for potential therapeutic applications that address long-term chronic diseases, it is of interest to develop DNA-binding molecules that exhibit very long-lived complexes capable of modulating bioprocesses on timescales relevant to organism lifespans. In this endeavour, a symmetric tetramer (**9**) was designed that could selectively bind to 5'-GATAAGTACTTATC-3' in 1:1 stoichiometry amongst nearly 500 base-pairs in a minor-major-minor grove topology

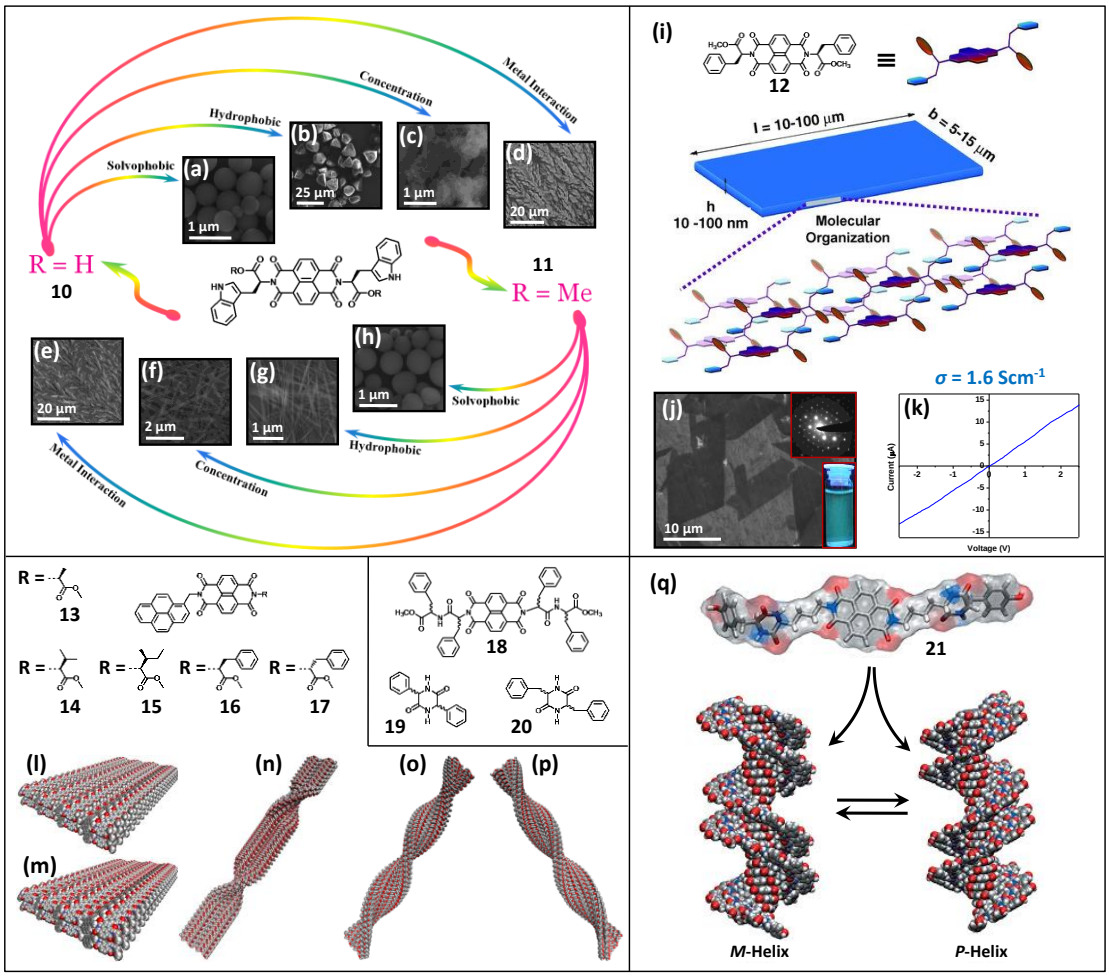

Fig. 5 Molecular structures of amino acid derivatives. (a-h) FESEM images of various self-assembled architectures obtained from **10** and **11**. Reproduced with permission of Royal Society of Chemistry from ref. 51. (i) Schematic representation of the two-dimensional (2D) sheets formed from **12**. (j) TEM image of the 2D nanosheets. Insets show the selected area electron diffraction and the excimer-like emission of the sheets. (k) Current-voltage curve recorded on the nanosheet show conductivity (σ) of 1.6 Scm^{-1}. Reproduced with permission of Wiley-VCH from ref. 52. (l-p) Molecular models show the self-assembly of **13**-**17** respectively. Reproduced with permission of Wiley-VCH from ref. 53. (q) Molecular models show the supramolecular helical assembly of **21**. Reproduced with permission of Wiley-VCH from ref. 57.

(Fig. 4m).[50] In addition, the dissociation of this tetra-intercalator complex was found to be extremely slow, corresponding to a half-life of 16 days, which is one of the longest half-lives ever reported for noncovalent complexes.

2.2 Nanomaterial applications

Recent works from our group and that of others have demonstrated that derivatization of amino acids with functional molecules serve as a versatile strategy to obtain advanced molecular materials.[4] In one of our earliest efforts, we illustrated that the assembly of a functional molecule like naphthalenediimide (NDI) could be tailored into various micro and nanoarchitectures by conjugating with tryptophan derivatives (**10**, **11**) upon utilization of various noncovalent interactions (Fig. 5a-h).[51] Following this, we reported the single crystalline two-dimensional (2D) assembly of an electroactive molecule like NDI by conjugating with phenylalanine methylester (**12**), which facilitated orthogonal π-π interactions (Fig. 5i, j).[52] These sheets exhibited the highest (for an undoped organic aggregate) known electrical conductivity of 1.6 Scm^{-1}, when probed using current sensing-atomic force microscopy (Fig. 5k). Moreover, it must be noted that NDI is a π-acidic molecule and forms self-sorted assemblies with π-basic molecule like pyrene.[53] However, our studies confirmed that dyads of NDI and pyrene could be tailored to undergo alternating stacking. Not only that, the so-formed charge transfer complexes could also be tailored into well-defined supramolecular architectures such as supercoiled helices, twisted nanoribbons, nanobelts, comb-edged nanoflakes and nanosheets, simply by incorporating minute structural mutations into the amino acid auxiliaries, **13**-**17** (Fig. 5l-p). We also demonstrated in a separate study that the inherent chiral information stored in the amino acids could be transcripted into supramolecular helical (*M* and *P*) assemblies of functional chromophores (**18**).[54] Interestingly, the nature of the helical assembly was found to depend upon the stereochemical

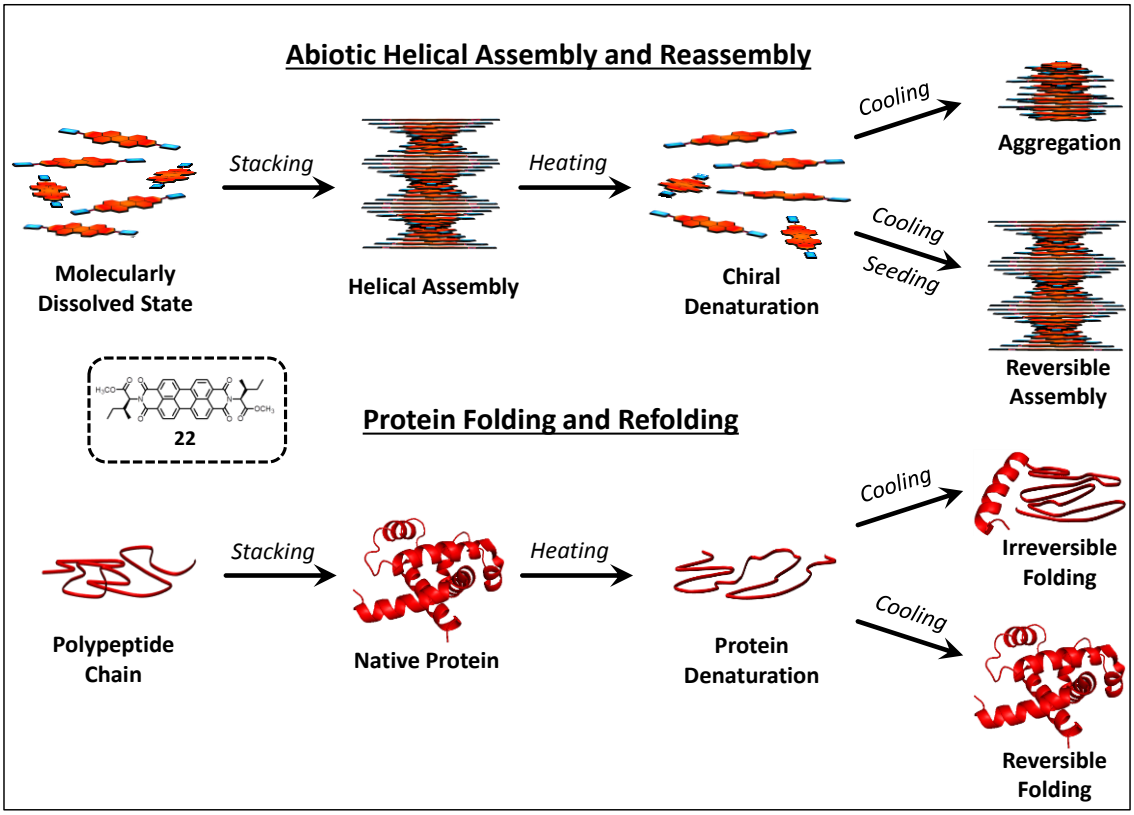

Fig. 6 Molecular structure of amino acid derivative. The schematic representation shows the relevance of the abiotic helical assembly and reassembly of **22** with the (secondary structure) protein folding and refolding. Reproduced with permission of American Chemical Society from ref. 58.

information, as well as the positions of amino acids with respect to the NDI chromophore. Specifically, we depicted that the nature (left- or right-handed) of supramolecular helicity of these chromophores was dictated by the stereochemistry of the amino acid adjacent to NDI and we have termed this unusual behaviour as 'retentive helical memory'. Moreover, by employing CDP (**19**, **20**) as model compounds, we confirmed that hydrogen-bonding interactions could be molecularly engineered to form 1D molecular chains, as well as 2D molecular layers, that in turn can form nano-, micro- and macroscopic structures.[55, 56] In addition, a reversible chiroptical switching between left and right-handed supramolecular helical assemblies of **21** was achieved by tuning the solvophobic interactions (Fig. 5q).[57] On the other hand, we found that isoleucine methylester functionalized perylene diimide (**22**) undergo extremely slow supramolecular helical assembly over a day's time. Interestingly, when these helical assemblies were subjected to heating and cooling cycles, irreversible trajectories (CD amplitudes) were observed for the first time and we have termed this transition as 'chiral denaturation'. These kinetically controlled assemblies could be made reversible only in the presence of non-denatured aggregates of **22**, which acts as seeds. This intriguing molecular assembly behaviour of **22** provided a rare opportunity to draw parallels with the secondary structure of proteins, envisaging its plausible implications in understanding the protein conformational diseases (Fig. 6).[58]

In an analogous approach, dipeptide-appended NDIs were assembled into amyloid-like 1D helical nanofibres and twisted nanoribbons, simply by employing a minimal alternating sequence of hydrophobic and polar residues.[59] On the other hand, the oligo(*p*-phenylenevinylene) conjugated to a silk-inspired *β*-sheet forming peptide resulted in 2D assemblies.[60] Detailed studies have confirmed that the packing of oligo(*p*-phenylenevinylene) was dictated both by the peptide segment and the formation of bilayers, wherein the molecules run antiparallel in a *β*-sheet conformation. Similarly, peptide-conjugated bithiophenes (**23**) were self-assembled into nanofibre-based self-supportive gels in completely aqueous and physiologically-relevant [Ca^{2+}] environments (Fig. 7a, b).[61] In a rational design, the self-assembling peptide amphiphiles capable of binding the metalloporphyrin was developed in order to provide photophysical functionality.[62] The peptide (**24**) capable of forming *β*-sheet structure also comprised of a histidine moiety so as to bind zinc protoporphyrin that ultimately propagated into large fibrous assemblies, which could be employed as scaffolds for light-harvesting fibres (Fig. 7c).

The self-assembly of a very short peptide, Alzheimer's *β*-amyloid diphenylalanine motif (**25**) resulted in the formation of discrete and stiff nanotubes.[63] These peptide nanotubes were

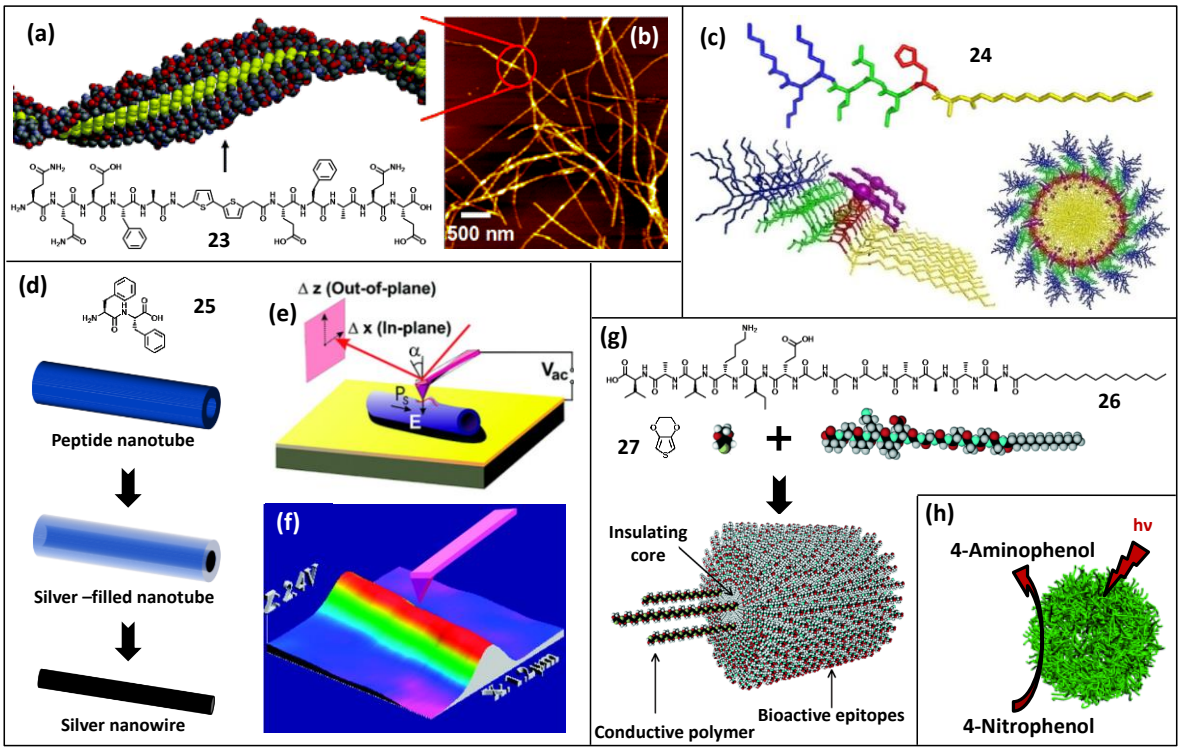

Fig. 7 Molecular structures of amino acid derivatives. (a) Schematic and (b) AFM image showing the formation of nanostructures from **23**. Reproduced with permission of American Chemical Society from ref. 61. (c) Molecular models show the structure of **24** and its assembly with Zinc-protoporphyrin (purple). Reproduced with permission of American Chemical Society from ref. 62. (d) Schematic representation of the casting of silver nanowires with the peptide nanotubes of **25**. Adapted with permission of American Association for the Advancement of Science from ref. 63. (e) Schematic of the in-plane measurements by piezoresponse force microscopy. (f) In-plane piezoresponse image of a single peptide nanotube. Reproduced with permission of American Chemical Society from ref. 64. (g) Proposed molecular model for the encapsulation of conductive polymer within the peptide architecture. Reproduced with permission of Wiley-VCH from ref. 67. (h) Schematic representation of the photocatalytic reduction by hybrid microspheres. Reproduced with permission of Wiley-VCH from ref. 69.

employed as moulds to cast metal nanowires (Fig. 7d). When the nanotubes were added to boiling ionic silver solution, silver nanowires were formed inside the nanotubes upon reduction with citric acid. Proteolytic cleavage of the peptide mould by the addition of proteinase K enzyme resulted in individual silver nanowires of ~20 nm diameter. Additionally, it was also demonstrated that these diphenylalanine peptide nanotubes exhibit high piezoelectric coefficient values of at least 60 pm V^{-1} (Fig. 7e, f).[64] Such piezoelectric (production of the electric field or charge under mechanical stress) nanomaterials find usage as 'green' acoustic transducers, sensors, actuators, peizomotors and more. In a separate study, Fmoc (9-fluorenylmethoxycarbonyl)-appended diphenylalanine peptide resulted in the formation of rigid gels in aqueous solutions.[65] This hydrogel was reported to be stable across a broad range of temperatures, over a wide pH range and even in the presence of chaotropic agents like urea and guanidinium hydrochloride. In an interesting design, collagen mimetic peptide that self-assembled with multi-hierarchical correlations was reported.[66] The designed peptide [(Pro-Lys-Gly)$_4$(Pro-Hyp-Gly)$_4$(Asp-Hyp-Gly)$_4$] comprised of collagen's characteristic proline-hydoxyproline-glycine repeating units as well as salt-bridged hydrogen bonds between lysine and aspartate to stabilize the triple helix into a sticky-ended assembly.

Redox-active supramolecular nanostructures find application as both biologically and electronically active matrices for the transduction of biological events.[67] For such applications, peptide amphiphiles (**26**) that self-assemble to cylindrical nanostructures were designed to uptake the hydrophobic conducting-polymer precursors within their hydrophobic core (Fig. 7g). By incorporating the hydrophobic 3,4-ethylenedioxythiophene (EDOT, **27**) monomers, followed by the addition of ammonium persulfate (chemical oxidant) resulted in the formation of conductive polymers (upon polymerization of EDOT) within the peptide nanofibres. In an another study, a straightforward method for the assembly of luminescent wires from semiconducting conjugated oligo-electrolytes, which were integrated into amyloid fibrils of bovine insulin was reported.[68] A separate study reported photocatalytically-active microspheres with highly hydrated and accessible multi-chambered interiors that were prepared by the cooperative assembly of dipeptides and porphyrins.[69] Under acidic conditions, the diphenylalanine peptide is in the form of a charged cation while the porphyrin derivative is anionic due to deprotonation of sulfonic acid groups. This electrostatically-induced assembly led to the formation of porous microspheres consisting of supramolecular J-type stacks of porphyrin molecules and, in turn, was found to render light harvesting

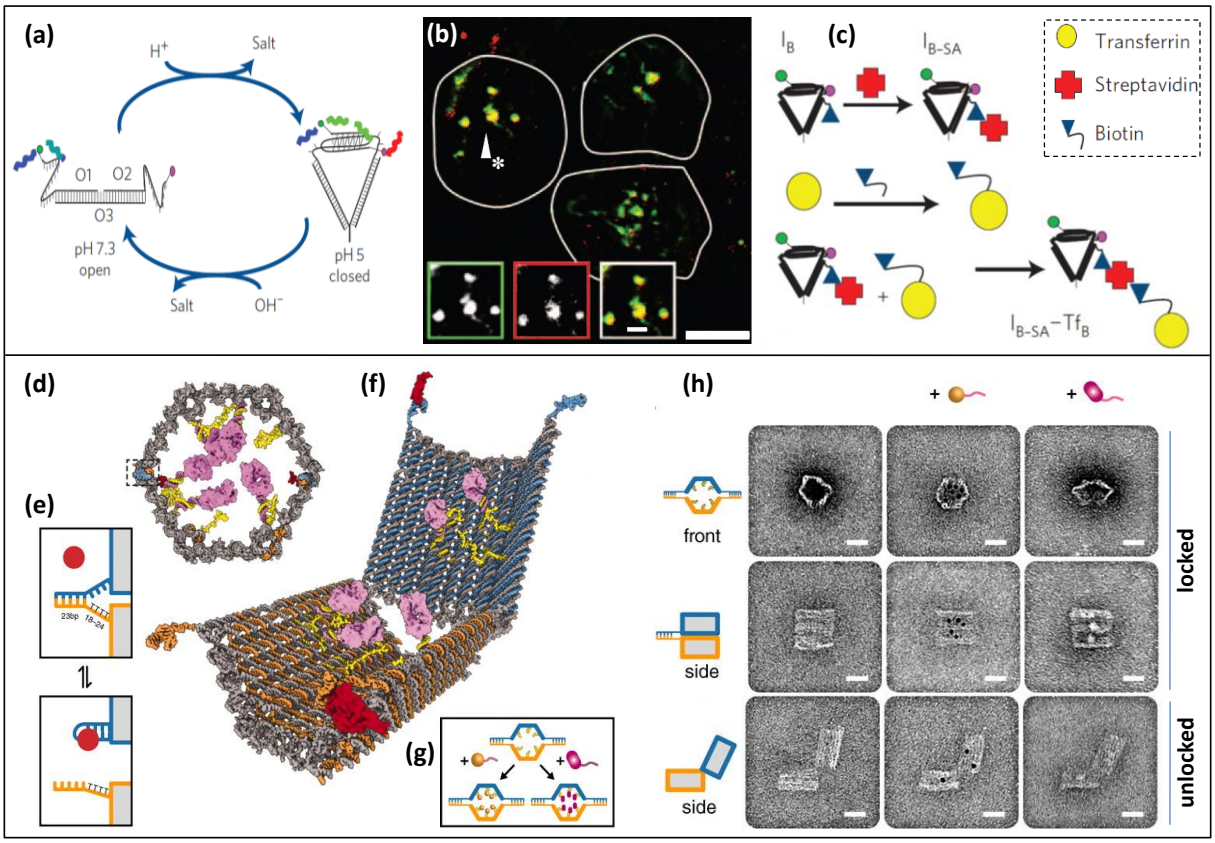

Fig. 8 (a) Schematic of the working principle of I-switch. (b) Confocal micrograph shows the internalization of I-switch and its function within endosomes of Drosophila haemocytes. I-switch (red) was co-localized with endocytic vesicle marker FITC-dextran (green). (c) Schematic showing the tagging of protein with the I-switch by employing transferrin, streptavidin and biotin. Reproduced with permission of Nature Publishing Group from ref. 73. (d) Schematic front view of closed nanorobot loaded with a protein payload. (e) A DNA aptamer (blue) and a partially complementary strand (orange) facilitate aptamer-based lock mechanism, wherein the antigen key (red) can stabilize the lock in its dissociated state. Schematic showing (f) the opened state of nanorobot and (g) a nanorobot loaded with payloads such as gold nanoparticles (gold) and antibody Fab' fragments (magenta). (h) TEM images of nanorobots in open and closed conformations, wherein left, centre and right columns represent unloaded, gold nanoparticles loaded and Fab' fragment loaded nanorobot, respectively. Scale bars, 20nm. Reproduced with permission of American Association for the Advancement of Science from ref. 80.

capability as well as photostability. Further, these microspheres were shown to act as a photosynthetic system for the photocatalytic reduction of 4-nitrophenol to 4-aminophenol (Fig. 7h).

3. Architectonics of functional nucleobases

Nucleobases are the nitrogen-containing heterocyclic biomolecules found in nucleotides, which are the basic building blocks of deoxyribonucleic acid (DNA) and ribonucleic acid (RNA). The important nucleobases are adenine, thymine, guanine, cytosine and uracil, abbreviated as A, T, G, C and U, respectively (Fig. 2). DNA comprises of A, T, G and C nucleobases while RNA possesses U instead of T. Further, in order to form the double helical structure of DNA, each type of nucleobase on one strand bonds non-covalently with only one type of nucleobase on the other strand, which is commonly known as (nucleo)base pairing. Herein, A binds only to T while G binds only to C *via* two and three hydrogen bonds, respectively. Due to this unique complementarity, all the information stored in the double-stranded sequence of DNA helix is duplicated on to each daughter strand during DNA replication and thereby the genetic information gets transferred. This reversible and specific noncovalent interaction between complementary base pairs has, thus, attracted enormous interest[70-72] amongst engineers, biologists and material scientists for its potential utilization in various nanotechnological applications as described below.

3.1 Nanobiological applications

DNA being the universal genetic material programs the functional aspects of almost all living organisms. However, the effective utilization of DNA-based nanomachines for *in vivo* applications was not reported until very recently.[73] These DNA nanomachines were reported to switch between defined molecular conformations upon stimulation by external triggers and were termed as I-switch (Fig. 8a). These nanomachines could be triggered by protons and function as a pH sensor (for the pH range of 5.5-6.8), based on fluorescence resonance energy transfer (FRET) inside living cells. The I-switch

consists of three oligonucleotides O_1, O_2 and O_3 that are hybridized to form a structure as shown in Fig. 8a. O_1 and O_2 possess single-stranded cytosine-rich overhangs that form one-half of a bimolecular i-motif. At acidic pH, protonated overhangs assemble to form an intramolecular i-motif. During the endosome maturation process a characteristic change of pH takes place from 6 to 6.2 in the early endosomes, to pH 5.5 in late endosomes and pH 5 in lysosomes. The I-switch was, therefore, employed to study the maturation of endosomes in *Drosophila* haemocytes (Fig. 8b). In addition, the I-switch conjugated to a protein of interest was also found to measure the pH of its environment (Fig. 8c). Further, it was demonstrated that these DNA nanomachines operate inside the nematode *Caenorhabditis elegans* as well.[74] In a remarkable extension to this approach, two distinct DNA nanomachines were simultaneously employed to map pH gradients along two different but intersecting cellular entry pathways.[75] These nanomachines, when delivered sequentially or simultaneously, probed the pH of early endosomes and the trans-Golgi network in real time within the same living cell.

Chemical functionalities presented by the self-assembled architectures play a crucial role in determining the outcome of several nanobiological applications.[76] This was believed to be feasible by employing low-molecular weight nucleobase-end capped monomers as a way to organize functional groups at the nanoscale. In an effort to illustrate this concept, guanine derivatives were employed considering their ability to interact with themselves or with complementary motifs through Watson-Crick and/or Hoogsteen binding. Triethylene glycol monomethyl ether groups (TEG) were attached to a tertiary amine, located at the centre of the hydrophobic core flanked by two guanine functionalities. These guanine derivatives were found to self-assemble into molecular monolayers in such a way that the TEG got grafted from the surface. These designer molecular assemblies exhibited reduced protein adsorption and platelet adhesion, as the grafted TEG aids in creating a hydrated layer. In a different report, enzyme-assisted catalytic dephosphorylation of adenosine monophosphate was developed to form supramolecular nanofibres that resulted in hydrogels.[77] These enzyme-catalyzed hydrogels were stated to serve as a novel type of soft biomaterials due to their exceptional selectivity, efficiency as well as *in vitro* and *in vivo* gelation capabilities.

With the advent of DNA origami technology, a wide variety of customized 2D and 3D assemblies have been made available.[78, 79] Such a methodology has been exploited to design an autonomous DNA nanorobot that can transport molecular payloads to cells.[80] A hexagonal barrel-shaped nanorobot was designed with dimensions of 35 nm × 35 nm × 45 nm (Fig. 8d-h). In a one-pot reaction, 196 oligonucleotide staple strands directed a 7308-base filamentous phage-derived scaffold strand into its target shape during a thermal annealing ramp of rapid heating followed by slow cooling. These DNA nanorobots could be loaded with a variety of materials at predetermined positions and were controlled by an aptamer-encoded logic gate, enabling them to respond to external cues. In another report, an autonomous molecular computer was developed that logically analyses the levels of messenger RNA species and, in response, produces a molecule capable of affecting the levels of gene expression.[81] This molecular computer was found to operate at a concentration of close to a trillion computers per microlitre and comprised of three programmable modules, namely, a computational module, an input module and an output module. Such examples which involve biomolecules as input data and biologically active molecules as outputs enable the production of programmable systems for effective control of biological processes.

3.2 Nanomaterial applications

The primordial property of nucleobases to form hydrogen-bonded molecular structures have been the driving force behind the exploration of their efficacy to achieve controllable molecular assemblies *via* the bottom-up approach.[82] Particularly, π-conjugated molecules are covalently attached to nucleobases/DNA for their precise organization at the nanoscale. For example, guanosine-conjugated oligothiophenes form 1D conjugated array due to hydrogen bonding between guanine nucleobases that dictate the spatial localization of oligothiophenes.[83] Instead of mononucleosides, single-stranded DNA has also been used as a template to obtain supramolecular stacks of chromophores *via* complementary hydrogen bonds.[84] Specifically, utilization of oligothymine strands resulted in complementary hydrogen bonds with diamino triazine unit-functionalized chromophores [e.g. oligo(*p*-phenylenevinylene) (**28**), and naphthalene (**29**)] (Fig. 9a). However, the complex of oligothymine and diamino triazine unit-functionalized naphthalene was found to be less stable than that of oligothymine and oligoadenine. Similarly, oligo(*p*-phenylenevinylene) appended with two nucleobases (**30**) on its either sides were shown to form hydrogen-bonded 1D nanostructures upon interacting with the complementary nucleobases of two single strands of DNA (Fig. 9b).[85] Likewise, chromophores such as NDI, porphyrin, pyrene, phenylethylene, distyrylbenzene and others were reported to be templated on DNA strands to form functional nanoassemblies.[86, 87] Besides chromophores, functional peptides have also been templated on double-stranded DNA that resulted in filamentous virus-like particles.[88] The functional peptide (**31**) was a triblock molecule that comprised of a spermine unit (nucleic acid ligand), a coiled-coil peptide (that aggregates into heptameric structures) and a polyethylene glycol unit (that provides solubility in water). These triblock moieties self-assembled to form mushroom-shaped capsomer-like nanostructures (Fig. 9c). Further, electrostatic interactions between the positively charged spermine units of the triblock and the negatively charged DNA resulted in monodisperse filamentous 1D aggregates (Fig. 9c). In an analogous approach, we had employed peptide nucleic acids (PNAs; **32** and **33**) as they form complexes with complementary nucleobase sequences with greater affinity and strength than the natural oligonucleotides.[89] Herein, NDIs appended with adenine (**34**) as

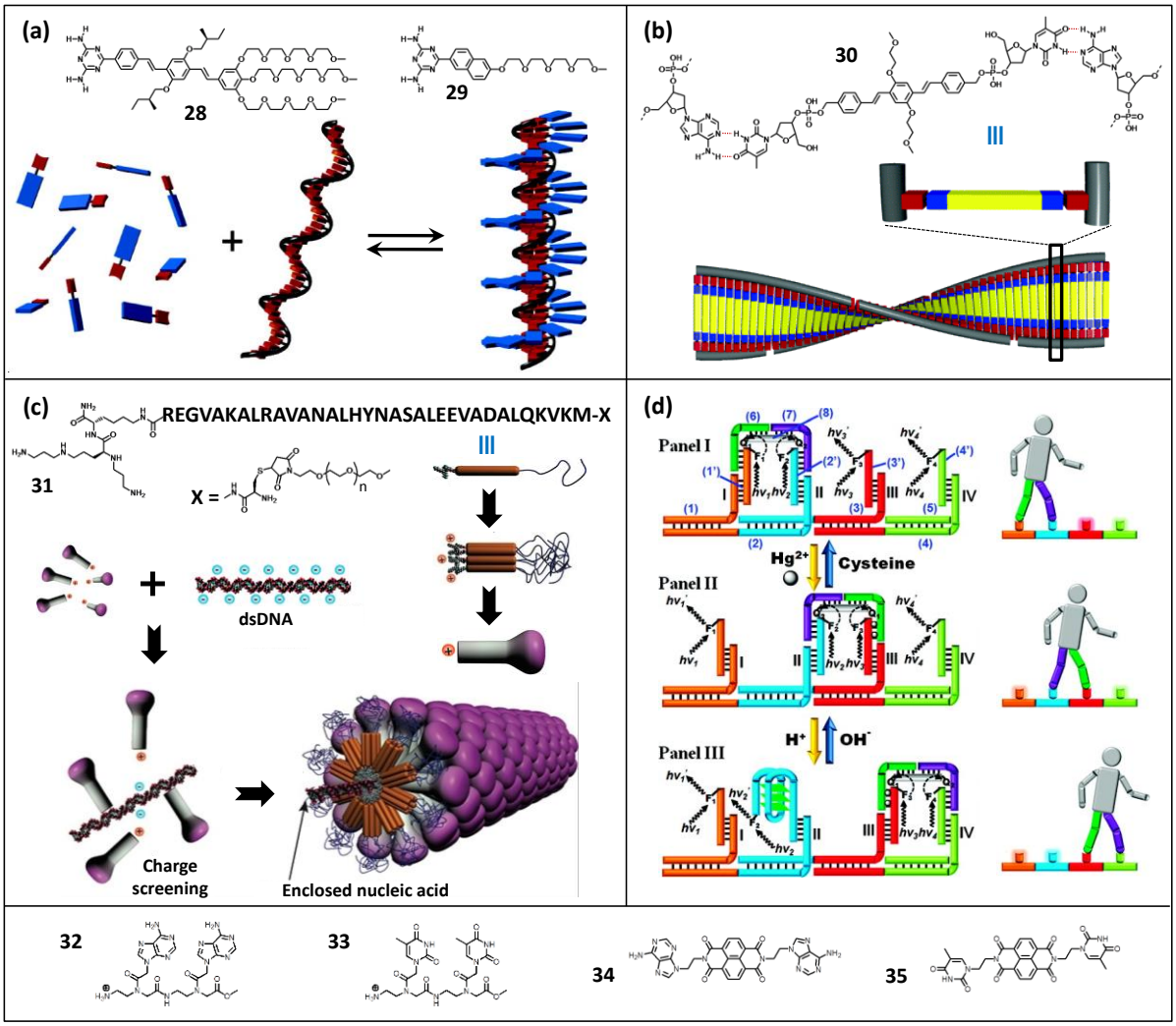

Fig. 9 Molecular structures of nucleobase derivatives. (a) Schematic representation of ssDNA (black strand) templated self-assembly of hydrogen-bonding unit (red bar) functionalized chromophores (blue bar). Reproduced with permission of American Chemical Society from ref. 84. (b) Proposed model for the self-assembly of **30** on two ssDNAs. Reproduced with permission of American Chemical Society from ref. 85. (c) Proposed model for the self-assembly of cationic spermine terminated peptides on dsDNA. Reproduced with permission of American Chemical Society from ref. 88. (d) Schematic representation of a bipedal walker activated by Hg^{2+}/cysteine and H^{+}/OH^{-} inputs. The walker is immobilized on footholds I and II in panel-I; footholds II and II in panel-II; footholds III and IV in panel-III. Reproduced with permission of American Chemical Society from ref. 96.

well as thymine (**35**) nucleobases were templated on complementary PNA clippers that resulted in well-defined architectures. In addition, it represented a unique example due to the involvement of both Watson-Crick and Hoogsteen type hydrogen bonding in case of adenine nucleobases.

Due to the presence of chiral deoxyribose moieties, the DNA strand can act as a chiral host template for the supramolecular helical organization of achiral guest chromophores. When diaminotriazine-equipped naphthalene guest derivatives were templated on oligothymine, right-handed organization of dye guests was observed.[90] However, the supramolecular helicity of this DNA-templated assembly was found to reverse due to protonation of guests. Also, multichromophoric 1D stacks are interesting nanostructures for functional optoelectronic applications that require efficient electron and/or energy transfer processes. For such applications, energy transfer between the supramolecular strand of donor guest (naphthalene) molecules and the cyanine dye acceptor, which was covalently attached to 5' end of a DNA strand, was demonstrated.[91] The efficiency of energy transfer was found to reach a maximum at templated stacks of 30 bases. Similarly, energy transfer process was also achieved in a DNA-templated zipper array of mixed porphyrin chromophores.[92] In another report, DNA-based light-harvesting antenna was developed that consisted of an array of stacked phenanthrene chromophores for collecting light, while exciplex-forming pyrene served as energy-collection centres.[93]

Lately, a DNA nano-spring that can perform spring-like motions with controllable functions has been developed.[94] The nano-spring powered by protons was prepared by assembling circular DNA and i-motif-forming oligonucleotides. This proton-fuelled nano-device was highly robust, reversible and

did not suffer from permanent deformations, as a real spring. Moreover, the fast response times as well as the absence of any side products that could poison the system were the added advantages. In another example, a synthetic molecular motor capable of autonomous nanoscale transport in solution was reported.[95] The autonomous locomotion was achieved by harnessing hybridization chain reaction, wherein the metastable DNA hairpins polymerize non-covalently when they encounter a target molecule. As per another study, a DNA-based bipedal walker was described, which could be activated by H^+/OH^- and Hg^{2+}/cysteine triggers (Fig. 9d).[96] The forward walking of the DNA on the template (that consisted of four nucleic acid footholds) was activated by Hg^{2+} ions and H^+ ions that resulted in thymine-Hg^{2+}-thymine complexation or the formation of i-motif structure. These DNA translocation driving forces were destroyed by OH^- ions and cysteine, and thereby aided in backward walking.

4. Architectonics of functional carbohydrates

Carbohydrates are polyhydroxy aldehydes/ketones and, in general, possess an empirical formula of the form $(CH_2O)_n$ [where *n* is three or more] (Fig. 2). Carbohydrates are further classified into four groups, namely, monosaccharides, disaccharides, oligosaccharides and polysaccharides. The monosaccharides (e.g. glucose, fructose) and disaccharides (e.g. sucrose, lactose) are commonly referred to as sugars. Carbohydrates and their derivatives play important roles as structural components (e.g. cellulose, chitin) and energy reservoirs (e.g. starch, glycogen) besides other roles in inflammation, immunological response, cell-cell recognition, blood clotting, and metastasis.[9, 10] Due to these key characteristic features of carbohydrates, efforts have been made to develop their functional derivatives for various implications.[97] However, the great strides in the field of carbohydrate research have been relatively slow considering associated difficulties with respect to synthesis, as well as isolation from cells. Nevertheless, some of the very few successful efforts in this endeavour form the basis of this section on functional carbohydrates for nanotechnological applications.

4.1 Nanobiological applications

The carbohydrate-protein interactions are one of the primary steps that trigger a series of biochemical processes leading to biological functions.[98] Understandably, these interactions are rather low-affinity, and in order to overcome this disability, nature adopts a design strategy involving multivalent systems. Cell surfaces are often decorated with glycoconjugates, which facilitate multivalent interactions with cell surface receptors and start a cascade of processes that can lead to cell attachment, fusion and others. For such objectives, fullerenes were utilized as spherical scaffolds that could be functionalized with any sugar of choice to modulate biochemical processes.[99] Specifically, when mannose (twenty four) groups were functionalized to the fullerene core (**36**), it was recognized by concanavalin A (lectin) in a multivalent manner, whereas galactose derivatives acted as a negative control. Similarly, multivalent presentation of glycodendrimers resulted in the blocking of C-type lectin, DC-SIGN, which recognizes glycoconjugates present on the surface of several pathogens.[100] A strong inhibitory activity with IC_{50} in the nanomolar range was achieved in a pseudotyped Ebola viral particles infection model. The cholera toxin is another example of a multivalent protein capable of binding carbohydrate moieties of five GM1 gangliosides simultaneously.[101] The designed dendritic scaffolds comprising multivalent GM1-oligosaccharides (**37**) acted as highly effective inhibitors for the cholera toxin B pentamer. Remarkably, these dendritic inhibitors had about 47500-fold more potency per GM1-oligosaccharide than a monovalent GM1-oligosaccharide conjugate. In another report, it was shown that multivalent GM1-inhibitors with mismatched valencies could operate *via* protein aggregation.[102] Moreover, the valency of the inhibitor was found to play a key role in determining the mechanism and kinetics of aggregation, as well as the stability of intermediate protein complexes.

Recently, antivirulence has emerged as an alternative chemotherapeutic strategy to combat microbial infections.[103] For example, the uropathogenic strain of *E. coli* that causes urinary tract infections exploit FimH, an adhesin overexpressed at the tip of their pili, to bind terminal mannose moieties found at the surface of the host epithelial cells. The designed synthetic mimic, fullerene hexakis-adducts bearing 12 peripheral mannose moieties was found to function as an effective ligand of the bacterial adhesin FimH. Interestingly, each of these fullerene scaffolds was found to accommodate as many as 7 FimH molecules. Another example is that of an opportunistic pathogen *Pseudomonas aeruginosa* that causes lethal airway infections in cystic fibrosis and immuno-compromised patients, wherein the formation of biofilms plays an important role in antibiotic resistance and disease progression.[104] This biofilm formation has been found to be mediated by the galactose-specific lectin LecA (PA-IL) and the fucose-specific lectin LecB (PA-IIL). β-phenylgalactosyl peptide dendrimer was recently developed to inhibit the *Pseudomonas aeruginosa* biofilm formation by specifically targeting the galactose-specific lectin LecA, whereas fucosylated glycopeptide dendrimer specifically targeted LecB. In an interesting development, a specific class of poly-amido-saccharide prepared by a controlled anionic polymerization of β-lactam monomers derived from either glucose or galactose was found to promote (**38**) as well as inhibit (**39**) the biofilm formation of *Pseudomonas aeruginosa* (Fig. 10a).[105] Likewise, calix[4]arene-based glycoconjugates strongly inhibited the binding of PA-IL to galactosylated surfaces for potential applications as anti-adhesive agents.[106]

One of the major reasons for malarial mortality is an inflammation cascade initiated by a malarial toxin, released when parasites rupture the host's red blood cells.[107, 108] Glycosylphosphatidylinositols (GPI) has been demonstrated to

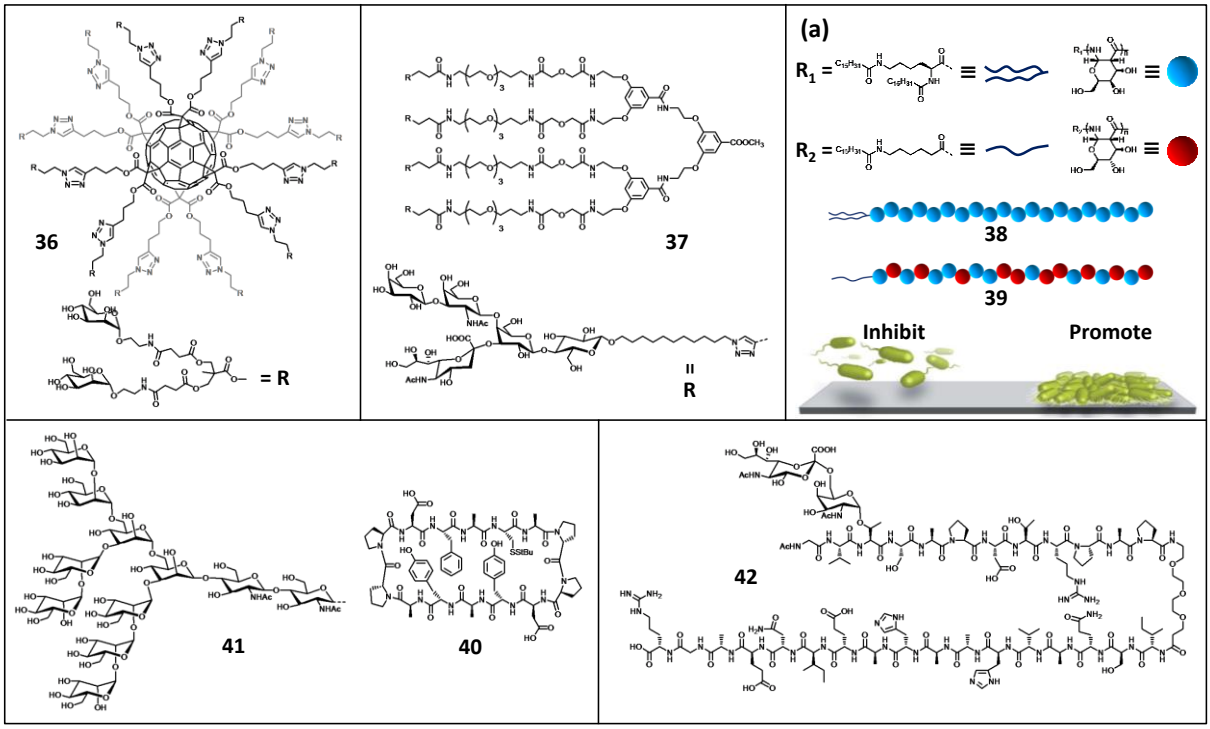

Fig. 10 Molecular structures of sugar derivatives. (a) Schematic representation shows the biofilm inhibition and promotion by poly-amido-saccharide amphiphiles. Reproduced with permission of Royal Society of Chemistry from ref. 105.

be a malarial toxin. Besides, it has also been demonstrated that anti-GPI vaccination can prevent malarial pathology in the animal model. In order to aid in this venture, malarial toxins were synthesized rapidly by an automated solid-phase oligosaccharide synthesizer, thereby paving the way, both to previously tested and next-generation vaccines. In another report, synthetic carbohydrate-based HIV antigens were developed based on the logic of the 2G12 antibody, which binds to an 'immunologically silent' region and is capable of neutralizing a broad range of HIV strains.[109] The designed CDP scaffold (**40**) consisted of D-Pro-L-Pro sequences to promote β-turns at both ends of the macrocycle and also presented side chains above as well as below the plane of the macrocycle that could be functionalized with glycans (**41**) and carrier proteins or biological markers. Similarly, a fully synthetic vaccine (**42**) consisting of tumour-associated sialyl-Tn glycopeptides antigen from MUC1 and a T-cell epitope from ovalbumin resulted in a highly specific humoral response against the tumour-associated structure.[110]

4.2 Nanomaterial applications

As emphasized earlier (section 4.1), carbohydrate-based biological signalling networks rely on avidity (strength of multiple interactions) rather than affinity (strength of a single interaction) due to their weaker interactions. With this knowledge, a multivalent probe comprising of a fluorescent ruthenium (II) core surrounded by heptamannosylated β-cyclodextrin scaffolds (**43**) was developed as a biosensor.[111] By employing these mannosylated epitopes, the *E. coli* strain ORN178 was observed under confocal microscopy by taking advantage of the fluorescent properties of ruthenium (II). Thus, user-friendly bacteria sensors can be envisaged with suitable carbohydrate epitopes. In another report, a cantilever array biosensor was designed to detect clinically relevant carbohydrate-protein interactions, which were reliable, sensitive, selective and reusable.[112] This sensor could detect picomolar quantities of cyanovirin-N, an oligomannoside-binding antiviral protein. Cyanovirin-N binding to immobilized oligomannosides on the cantilever resulted in mechanical surface stress that was transduced into a mechanical force and cantilever bending, which could be correlated with the binding interactions, their strength and molecular binding preferences. This cantilever-based sensor was also employed for the real-time detection of several *E. coli* strains in suspension.[113]

In a separate study, perylene bisimides (**44**) containing D-mannose as chiral auxiliaries resulted in highly water soluble derivatives with an interesting solvent-dependent supramolecular helical assembly (Fig. 11a).[114] Up to 60% v/v proportion of water in water-dimethylsulfoxide solvent composition, these perylene bisimides assemble into left-handed supramolecular helices, while for more than 85% v/v proportion of water in water-dimethylsulfoxide, right-handed helices were obtained. Amphiphilic homoglycopolypeptides were reported, wherein poly-L-glutamate backbone was grafted with glucose side chains that consisted of hydrophilic –OH groups and one hydrophobic $-C_6H_{13}$ group.[115] These amphiphilic glycopolypeptides self-assembled in water to form

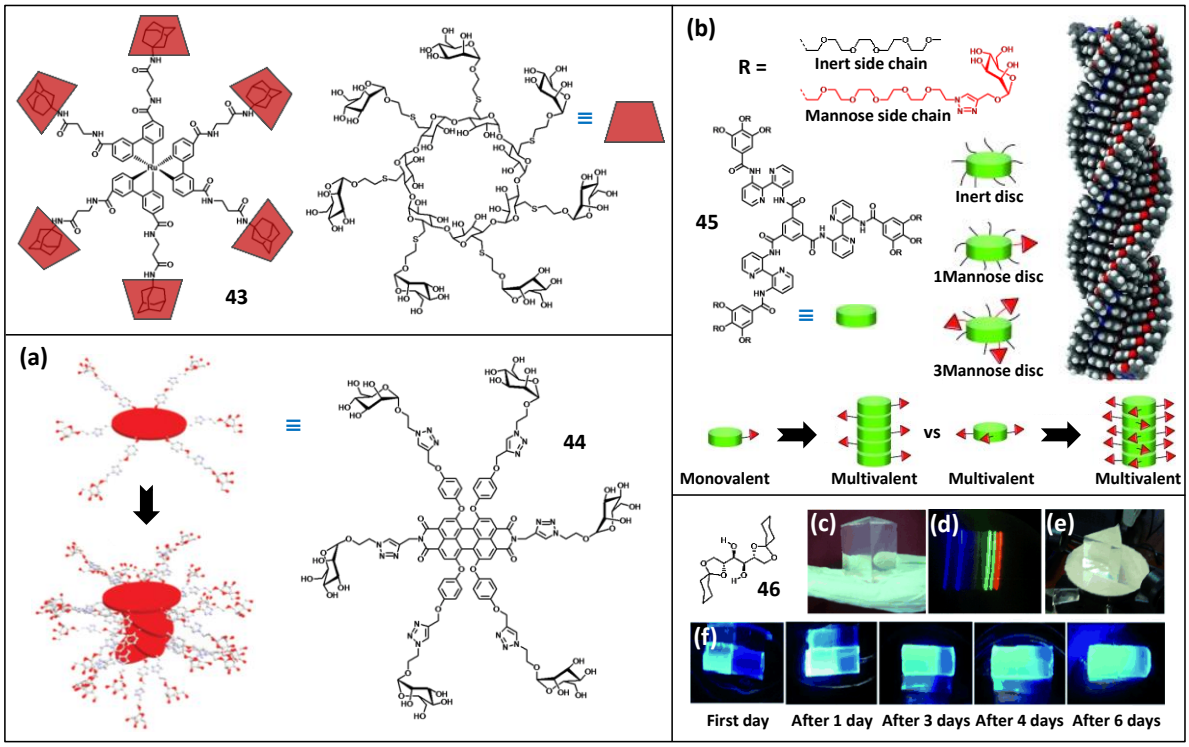

Fig. 11 Molecular structures of sugar derivatives. Schematic representation shows the self-assembly of (a) **44** and (b) **45** and the latter exhibits the self-assembling multivalency attained from monovalent discotic molecules. Reproduced with permission of (a) Royal Society of Chemistry from ref. 114 and (b) Wiley-VCH from ref. 116. (c) Photograph of pump oil based gel prism. (d) Photograph of gel prism based diffraction pattern and that placed on a spectrometer table (e). (f) A pyrene-doped gel fused to an undoped gel shows the gradual exchange of pyrene with the undoped region. Reproduced with permission of Wiley-VCH from ref. 122.

multimicellar aggregates of about 250 nm diameter. Due to the presence of hydrophobic and hydrophilic domains, dyes like calcein (hydrophobic) and nile red (hydrophilic) were found to be incorporated within the multimicellar nanoarchitectures.

Monovalent building blocks decorated with a single bioactive ligand (**45**) were designed to self-assemble into columnar polymers that display multiple ligands (Fig. 11b).[116] Remarkably, these self-assembled architectures exhibited a stronger inhibitory power than that of the monovalent bioactive ligands. This bottom-up approach termed as 'self-assembling multivalency' enables the rapid and flexible generation of multivalent polymers from monovalent building blocks. In another development, a novel integrated supramolecular device based on a helical carboxymethyl amylose was reported as an artificial photosynthetic mimic.[117] This amylose was stated to act as a host for J-aggregation of cyanine dyes onto the helical surface and also for the inclusion of donor-acceptor chain chromophores inside the helical cavity. Herein, the J-aggregates functioned as an array of photoreceptor antenna that funnel excitation across the helix to the donor-acceptor chromophores, which functions as reaction centres.

A naphthalene molecule containing the unnatural amino acid [3-(2-naphthyl)-alanine], when conjugated to nucleobase-saccharide-amino acid residues, resulted in hydrogelation.[118] This example illustrates a facile strategy for generating bioactive and functional hydrogelators from the basic biological building blocks. These functional hydrogelators also find importance because the naphthalene-containing unnatural amino acid residues have served as antagonists, inhibitors and catalysts. Integration of glucosamine with nucleobases and RGD peptides also engendered supramolecular hydrogelation.[119] Incorporation of RGD peptides was reported to enable the hydrogels with an inherent functionality to bind live cells while the self-assembled glycoside residues mimic the polysaccharides that are the important components of extracellular matrices. Aromatic carbohydrate amphiphiles driven by CH-π interactions and T-stacking of fluorenyl groups were also found to form supramolecular hydrogels.[120] Another study reported the conjugation of azobenzene to disaccharides that resulted in photosensitive hydrogelators with reversible gel-sol transitions.[121] Remarkably, lactose-azobenzene moiety rendered (*R*)-chirality for the supramolecular aggregate while the maltose-azobenzene conjugate exhibited (*S*)-chirality and cellobiose-azobenzene derivative existed in an achiral form. This suggests that the glycosidic linkages and the steric arrangement of hydroxyl groups in the conjugated carbohydrates influence the helical organization of chromophores. Unlike the hydrogelators discussed so far, a simple D-mannitol-based sugar (**46**) was found to gelate nonpolar solvents and oils by means of intermolecular hydrogen bonding.[122] These oil gels were found to be strong, highly transparent, self-healing and possessed glass-like

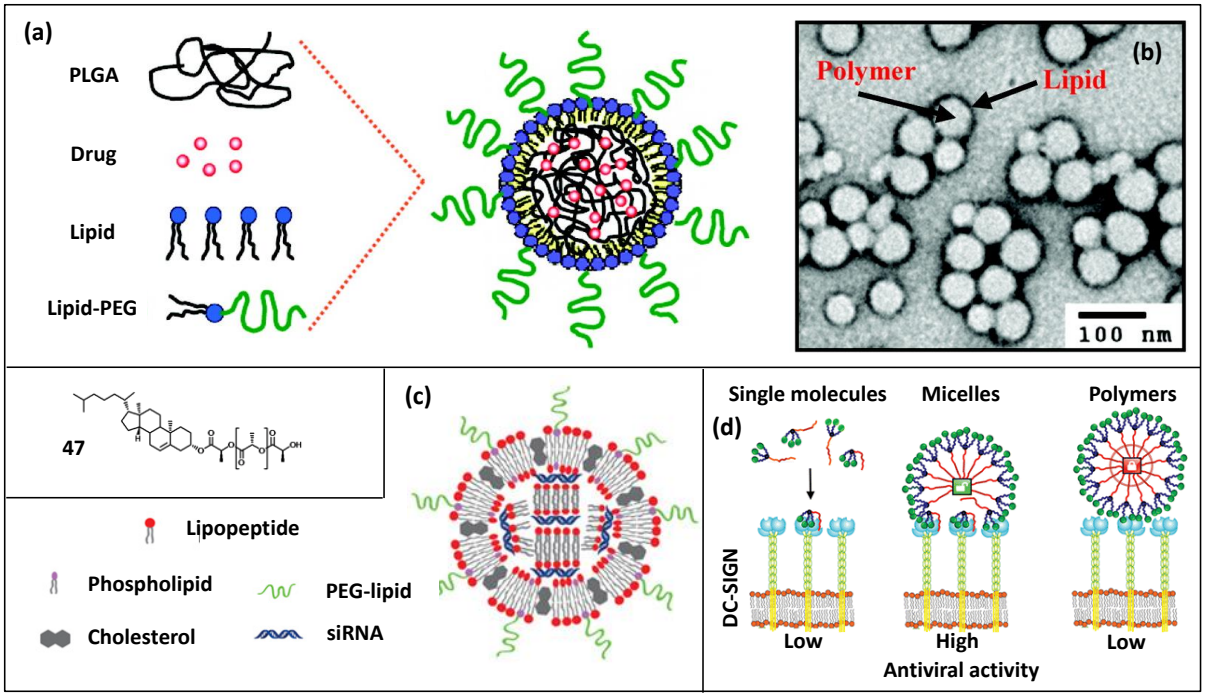

Fig. 12 Molecular structure of lipid derivative. (a) Schematic representation depicts the formulation of lipid-polymer hybrid nanoparticles. Reproduced with permission of American Chemical Society from ref. 123. (b) TEM image of lipid-polymer hybrid nanoparticles. (c) Proposed model of a lipopeptide based nanoparticles. Reproduced with permission of National Academy of Sciences (USA) from ref. 125. (d) Schematics show the high antiviral recognition exhibited by dynamic micelles. Reproduced with permission of American Chemical Society from ref. 129.

refractive indices besides high visible-light transmittance (Fig. 11c-e). These unusual properties were employed to fabricate soft optical devices like double convex gel lens, planoconvex gel lens, gel prism and gel UV-filter. Moreover, when a pyrene-doped gel was fused with an undoped gel, diffusion of pyrene to undoped gel was observed (Fig. 11f). This suggested the dynamic exchange of dissolved molecules across the fusion interface and thereby facilitated the self-healing process.

5. Architectonics of functional lipids

Lipids are the naturally occurring small hydrophobic or amphiphilic molecules that include fats, waxes, sterols, glycerides and others (Fig. 2). Lipids can be classified into different categories such as fatty acids, glycerolipids, glycerophospholipids, sphingolipids, saccharolipids, polyketides, sterol lipids and prenol lipids. Lipids contribute to important biological functions such as energy storage, signalling and as structural components of cell membranes. A biological membrane is a form of energetically-favoured lipid bilayer produced due to hydrophobic effect in an aqueous environment. The amphiphilic lipid molecules are organized in a way that the polar heads of the lipids align towards the aqueous environment while the hydrophobic tails get buried in order to minimize their exposure to water.[11] Depending on the concentration and the dimensions of the conical shape of the lipid molecule, they form micelles, liposomes, cylindrical fibres or bilayer sheets. Especially, these latter attributes have enabled lipid derivatives for various nanotechnological applications.

5.1 Nanobiological applications

The limitations of conventional drug delivery approaches such as high toxicity, high dosage, *in vivo* degradation and short circulating half-lives have attracted tremendous interest towards targetable nanotherapeutic systems.[15] In this context, lipid-polymer hybrid nanoparticles were designed to facilitate a robust drug delivery platform with high drug encapsulation yield, tuneable and sustained drug release profile, excellent serum stability and the potential for differential targeting of cells or tissues (Fig. 12a, b).[123] These hybrid nanoparticles are comprised of three distinct functional components: 1) a hydrophobic polymeric core to encapsulate poorly water-soluble drugs; 2) an antibiofouling hydrophilic polymeric shell to enhance nanoparticle stability and systemic circulation, and 3) a lipid monolayer at the interface of the core and the shell that acts as a molecular fence to regulate the retention as well as controlled release of drugs. Ester-terminated poly D, L-lactic-*co*-glycolic acid (PLGA), polyethylene glycol (PEG) and lecithin were employed as the hydrophobic polymer (that forms the core of the nanoparticle), hydrophilic polymer (that forms the 'stealth' shell of the nanoparticle) and a model lipid (that forms the interface of nanoparticle core and shell), respectively. In another report, paclitaxel-loaded lipid-polymeric nanoparticles that were surface-functionalized with collagen IV-targeting peptides resulted in the antiproliferation of injured

vasculature and also led to ~50% reduction in arterial stenosis when compared to sham-injury group.[124] In another report, lipopeptide-based nanoparticles were also developed as small interfering RNA (siRNA) carriers, which is a promising approach for the treatment of a wide variety of genetic disorders (Fig. 12c).[125] The siRNA-lipopeptide nanoparticles provided the most potent and selective *in vivo* delivery to hepatocytes in mice. In addition, these nanoparticles also silenced multiple genes in three different animal species, inducing transthyretin silencing of over 95% in cynomolgus monkeys.

Cholesterol-based liquid crystals (**47**) were designed to interact with cells and to serve as scaffolds for tissue regeneration.[126] Cholesterol was chosen due to its universal affinity for cell membranes while a short chain of lactic acid was employed as it is one of the most common components of biodegradable tissue engineering matrices. These self-assembled layered structures of cholesteryl derivatives were found to promote improved fibroblast adhesion and spreading. Moreover, it was shown that a physical mixture of polylactic acid and cholesterol resulted in phase separation and induced cytotoxicity due to elevated levels of dissolved cholesterol. Also, the self-assembled multilayers of cholesteryl-lactic acid derivative were reported to offer the possibility of sustained controlled release of cholesterol for enhanced bioactivity. The cell surface of an extreme thermophile, *Thermus thermophilus* possesses very unique phosphoglycolipids that comprise of a glucosamine moiety and a phosphatidyl group connected to each other by the α-glycosidically-linked glyceric acid long-chain amide.[127] These phosphoglycolipids and their analogues that were synthesized artificially for the first time showed their apparent immunostimulatory activity.

The pathogenicity and virulence of Gram-negative bacteria that cause a variety of infectious diseases such as meningitis, pneumonia and plague are often associated with the lipopolysaccharide coat.[128] For a better understanding of their role in host-pathogen interactions and to elucidate the antigenic/immunogenic properties of lipopolysaccharides, a well-defined collection of inner core oligosaccharides are required. In this venture, a diversity-oriented approach was undertaken recently to synthesize a range of lipopolysaccharide inner core oligosaccharides from a variety of pathogenic bacteria including *Yersinia pestis*, *Haemophilus influenzae* and *Proteus*. In another report, it was shown that mannoside glycolipid conjugates inhibit human immunodeficiency virus type 1 (HIV-1) *trans*-infection mediated by human dendritic cells.[129] The designed conjugates consisted of a linear or branched mannose head, a hydrophilic linker and a 24-carbon lipid chain. In order to optimize the effect of supramolecular architectures on the inhibitory activity, a comparison between single molecules, dynamic self-assembled micelles and photopolymerized cross-linked polymers were employed (Fig. 12d). This exercise showed that HIV-1 *trans*-infection was mostly inhibited by dynamic micelles and not by rigid polymers. Further studies revealed that trivalent glycolipid conjugates display the highest microbicide potential for HIV prophylaxis.

5.2 Nanomaterial applications

Lately, ferroelectric materials have attracted tremendous interest due to their potential applications in ferroelectric random-access memories (FERAM), ferroelectric field effect transistors (FEFET), ferroelectric diodes and multiferroic materials. Unlike inorganic counterparts, all-organic ferroelectric materials enable several advantages such as synthetic tailorability, tunability of molecular interactions and solution processability.[130] The designed steroid-conjugated donor-π-acceptor molecules (**48**-**50**) showed spontaneous polarization both in the form of single crystals (For **48**, *P*s: 0.614 $\mu C\ cm^{-2}$) as well as self-assembled nanoarchitectures (For **50**, *P*s: 0.498 $\mu C\ cm^{-2}$) at room temperature itself (Fig. 13a, b). This single-component ferroelectric molecule comprised of four modules, namely 1) mod-A: a nitroaniline-based donor-π-acceptor unit to attain spontaneous polarization; 2) mod-B: an enantiomerically pure steroid unit to aid in polar ordering; 3) mod-C: hydrogen bonding units to drive the self-assembly and 4) mod-D: a spacer unit to adjust and error-proof the packing between successive layers. In a separate report, a synthetically pure β-anomer glycolipid was found to exhibit a large pyroelectric coefficient of ~ 80 $\mu C\ m^{-2}K^{-1}$ under zero applied bias field.[131] Moreover, the induced polarization in this glycolipid thin film was found to be stable even at 100^{o}C.

Commercially available single-walled carbon nanotubes (SWNTs) were surface functionalized noncovalently with an archaeal glycolipid made of isopranoid alkyl chains.[132] The wrapping of glycolipids around the SWNTs was attributed to directional and cooperative CH-π hydrogen bonds. Additionally, these hybrid complexes resulted in electron transfer from the glycolipid to the nanotubes. On the other hand, amphiphilic glycolipids with an amide ligating the hydrophilic and hydrophobic parts of the amphiphile afforded micelles while those possessing a triazole formed nanotubes.[133] These nanotubes bundled together in a 3D network at higher concentrations to form hydrogels. Photopolymerization of these glycolipids resulted in the formation of conjugated poly(diacetylene) derivative, and thereby, rigidified nanomaterial was obtained. The extended π-delocalization along the polymerized nanotube rendered intense blue colouration. In addition, these nanotubes changed their colour to red as a consequence of heat or due to solvent effects and, thus, exhibited thermochromism or solvatochromism, respectively.

An amphiphilic glycolipid containing a disaccharide hydrophilic head and a palmitic acid chain as a hydrophobic tail showed liquid-crystalline as well as gelation properties.[134] Analogously, the supramolecular hydrogels formed from the bola-amphiphilic glycolipids (**51**) exhibited a naked-eye sensing property in response to temperature as well as to glycosidases (Fig. 13c).[135] This bola-amphiphilic glycolipid comprised of a π-conjugated chromophore at the centre with a

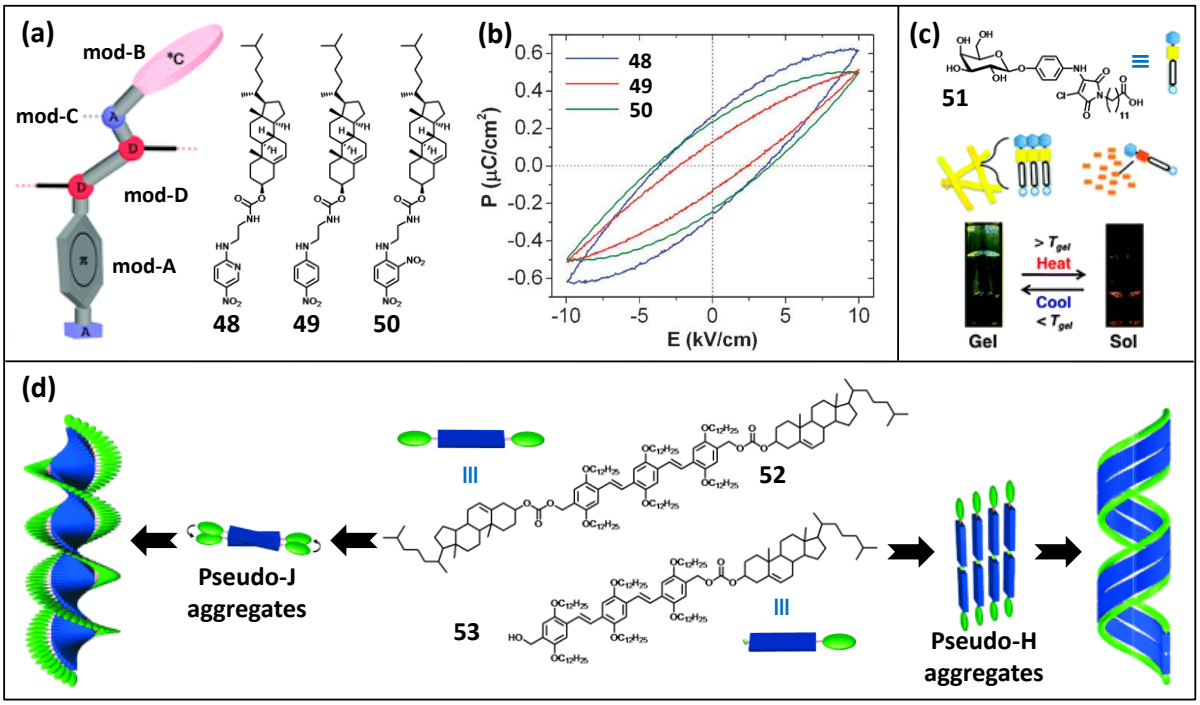

Fig. 13 Molecular structures of lipid derivatives. (a) Schematic representation shows the various modules (mod-A, mod-B, mod-C and mod-D) of steroid based molecules. (b) Electric hysteresis loops of **48**, **49** and **50** at room temperature. Reproduced with permission of Royal Society of Chemistry from ref. 130. (c) Photographs and schematics show the reversible thermal gel-to-sol transitions and thermochromism of **51**. Reproduced with permission of Royal Society of Chemistry from ref. 135. (d) Proposed molecular packing model for the self-assembly of **52** and **53** into twisted and coiled helices. Reproduced with permission of Wiley-VCH from ref. 136.

sugar (glucose/galactose/mannose) and carboxylic acid functionality as hydrophilic groups on its either sides. These thermoreversible hydrogels exhibited a yellow colouration in the gel state, and an orange colouration in the sol state. Additionally, this colour change was also observed by the addition of glycosidases that selectively cleave the glucosidic bond and thereby facilitate the transition from gel to sol state. In a separate study, symmetrical (di-substituted, **52**) and unsymmetrical (mono-substituted, **53**) functionalization of oligo(*p*-phenylenevinylene) with cholesterol allowed controlled supramolecular organization (Fig. 13d).[136] Interestingly, mono-substituted derivative resulted in coiled-helices with pseudo-J aggregates, whereas di-substituted derivative formed twisted helices possessing pseudo-H aggregates. Thus, it was demonstrated that simple structural modifications can bring about remarkable differences in optical, chiroptical, and morphological properties.

6. Conclusions and future outlook

In this Feature Article, with the aid of pertinent examples we illustrated that functional biomolecular engineering is a versatile strategy for various nanotechnological applications. Specifically, our discussions were centred on four important biomolecules *viz.*, amino acids, nucleobases, carbohydrates, and lipids for nanobiological and nanomaterial applications. Herein, we have provided a flavour of the design principles embraced as well as the kind of applications that are embarked upon, spanning from electronics to biomedicine. As these biomolecules possess distinct chemical functionalities, they inherit different properties, and, therefore, a wide variety of applications are at our disposal. In addition, such ventures are also likely to bring about deeper insights into the complex biochemical processes as well as aid in the development of synthetic biology field.

Over the years, the extensive investigations carried out by biochemists and molecular biologists has no doubt led us to understand the various biochemical processes, but it is the exploitation of this fundamental knowledge that is intended to form the essence of this emerging biomolecular engineering discipline. In doing so, first and foremost we can learn the very process of molecular designing and their pre-programmable assemblies that nature has mastered over billions of years of natural selection and evolution. In this regard, we are of the opinion that more efforts should be focused on envisaging the kinetically controlled assemblies, which find direct correlations to natural systems and are also quite complex to realize compared to thermodynamically controlled systems. Unlike the biomacromolecules, designer molecules would be relatively small and getting the right combination of hydrophilicity, hydrophobicity as well as the functional components within the kinetically controlled assemblies could be a significant challenge to embark on. Secondly, our primary understanding of biochemical processes can be put to test so as to enable us to device better methodologies for diagnostics, therapeutics and theranostics. Herein, thoughtfully designed systems that can

produce phenomenal selectivity, specificity and sensitivity are essential, while extending their performance to *in vivo* conditions could be a daunting task. Thirdly, biomolecular materials that are biocompatible, solution processable, economically viable, self-healable and self-assembled can be envisaged for a variety of applications pertaining to energy, health and environment. In this venture, primary efforts should be exerted on achieving the optimal performances of the designed biomolecular materials. Thus, it is apt to believe that by employing biomolecules in conjunction with the innumerable functionalities that can be imagined, countless implications for our day-to-day activities seem probable.

Acknowledgements

Authors thank Prof. C. N. R. Rao, FRS for constant support and encouragement, JNCASR, Innovative Young Biotechnologist Award grant (BT/03/IYBA/2010), Department of Biotechnology (DBT), Government of India for financial support, Sheikh Saqr Laboratory (SSL), ICMS, JNCASR for Sheikh Saqr Career Award Fellowship to T.G, and Defence Research and Development Organisation (DRDO) for RA fellowship to M.B.A.

Notes and references

[a]Bioorganic Chemistry Laboratory, New Chemistry Unit (NCU), Jawaharlal Nehru Centre for Advanced Scientific Research (JNCASR), Jakkur P. O., Bangalore 560064, India. Email: tgraju@jncasr.ac.in; Fax: +91 80 22082627; Tel: +91 80 22082969.

1. J. M. Zayed, N. Nouvel, U. Rauwald and O. A. Scherman, *Chem. Soc. Rev.*, 2010, **39**, 2806-2816.
2. S. I. Stupp, *Nano Lett.*, 2010, **10**, 4783-4786.
3. X. Zhao and S. Zhang, *Chem. Soc. Rev.*, 2006, **35**, 1105-1110.
4. M. B. Avinash and T. Govindaraju, *Adv. Mater.*, 2012, **24**, 3905-3922.
5. J. B. Matson, R. H. Zha and S. I. Stupp, *Curr. Opin. Solid State Mater. Sci.*, 2011, **15**, 225-235.
6. A. M. Kushner and Z. Guan, *Angew. Chem. Int. Ed.*, 2011, **50**, 9026-9057.
7. F. A. Aldaye, A. L. Palmer and H. F. Sleiman, *Science*, 2008, **321**, 1795-1799.
8. Y. Lu and J. Liu, *Curr. Opin. Biotechnol.*, 2006, **17**, 580-588.
9. C. R. Bertozzi, Kiessling and L. L., *Science*, 2001, **291**, 2357-2364.
10. D. B. Werz and P. H. Seeberger, *Chem. Eur. J.*, 2005, **11**, 3194-3206.
11. K. W. Ferrara, M. A. Borden and H. Zhang, *Acc. Chem. Res.*, 2009, **42**, 881-892.
12. Y.-Y. Luk and N. L. Abbott, *Curr. Opin. Colloid Interface Sci.*, 2002, **7**, 267-275.
13. K. Ariga, X. Hu, S. Mandal and J. P. Hill, *Nanoscale*, 2010, **2**, 198-214.
14. H. Tao, D. L. Kaplan and F. G. Omenetto, *Adv. Mater.*, 2012, **24**, 2824-2837.
15. K. Riehemann, S. W. Schneider, T. A. Luger, B. Godin, M. Ferrari and H. Fuchs, *Angew. Chem. Int. Ed.*, 2009, **48**, 872-897.
16. S. H. Kim and J. R. Parquette, *Nanoscale*, 2012, **4**, 6940-6947.
17. K. Ariga, M. Li, G. J. Richards and J. P. Hill, *J. Nanosci. Nanotechnol.*, 2011, **11**, 1-13.
18. K. Ariga, A. Vinu, Y. Yamauchi, Q. Ji, and J. P. Hill, *Bull. Chem. Soc. Jpn.*, 2012, **85**, 1-32.
19. K. Ariga, Y. Yamauchi, G. Rydzek, Q. Ji, Y. Yonamine, K. C.-W. Wu and J. P. Hill, *Chem. Lett.* 2014, **43**, 36-68.
20. T. Govindaraju and M. B. Avinash, *Nanoscale*, 2012, **4**, 6102-6117.
21. M. Ramanathan, L. Shrestha, T. Mori, Q. Ji, J. P. Hill and K. Ariga, *Phys. Chem. Chem. Phys.*, 2013, **15**, 10580-10611.
22. K. Ariga, Q. Ji, T. Mori, M. Naito, Y. Yamauchi, H. Abe and J. P. Hill, *Chem. Soc. Rev.*, 2013, **42**, 6322-6345.
23. K. Ariga, K. Kawakami, M. Ebara, Y. Kotsuchibashi, Q. Ji and J. P. Hill, *New J. Chem.*, 2014, DOI: 10.1039/C4NJ00864B
24. R. de la Rica and H. Matsui, *Chem. Soc. Rev.*, 2010, **39**, 3499-3509.
25. Y.-C. Yu, P. Berndt, M. Tirrell and G. B. Fields, *J. Am. Chem. Soc.*, 1996, **118**, 12515-12520.
26. N. Nakashima, S. Asakuma and T. Kunitake, *J. Am. Chem. Soc.*, 1985, **107**, 509-510.
27. N. Yamada, K. Ariga, M. Naito, K. Matsubara and E. Koyama, *J. Am. Chem. Soc.*, 1998, **120**, 12192-12199.
28. J. D. Hartgerink, E. Beniash and S. I. Stupp, *Science*, 2001, **294**, 1684-1688.
29. C. J. Newcomb, R. Bitton, Y. S. Velichko, M. L. Snead and S. I. Stupp, *Small*, 2012, **8**, 2195-2202.
30. A. Mata, Y. Geng, K. J. Henrikson, C. Aparicio, S. R. Stock, R. L. Satcher and S. I. Stupp, *Biomaterials*, 2010, **31**, 6004-6012.
31. E. D. Sone and S. I. Stupp, *Chem. Mater.*, 2011, **23**, 2005-2007.
32. D. J. Mooney and H. Vandenburgh, *Cell Stem Cell*, 2008, **2**, 205-213.
33. M. J. Webber, J. Tongers, M.-A. Renault, J. G. Roncalli, D. W. Losordo and S. I. Stupp, *Acta Biomater.*, 2010, **6**, 3-11.
34. M. J. Webber, J. Tongers, C. J. Newcomb, K.-T. Marquardt, J. Bauersachs, D. W. Losordo and S. I. Stupp, *Proc. Natl. Acad. Sci.*, 2011, **108**, 13438-13443.
35. L. W. Chow, R. Bitton, M. J. Webber, D. Carvajal, K. R. Shull, A. K. Sharma and S. I. Stupp, *Biomaterials*, 2011, **32**, 1574-1582.
36. G. A. Silva, C. Czeisler, K. L. Niece, E. Beniash, D. A. Harrington, J. A. Kessler and S. I. Stupp, *Science*, 2004, **303**, 1352-1355.
37. V. M. Tysseling-Mattiace, V. Sahni, K. L. Niece, D. Birch, C. Czeisler, M. G. Fehlings, S. I. Stupp and J. A. Kessler, *J. Neurosci.*, 2008, **28**, 3814-3823.
38. S. Sur, C. J. Newcomb, M. J. Webber and S. I. Stupp, *Biomaterials*, 2013, **34**, 4749-4757.
39. J. Kisiday, M. Jin, B. Kurz, H. Hung, C. Semino, S. Zhang and A. J. Grodzinsky, *Proc. Natl. Acad. Sci.*, 2002, **99**, 9996-10001.
40. R. N. Shah, N. A. Shah, M. M. Del Rosario Lim, C. Hsieh, G. Nuber and S. I. Stupp, *Proc. Natl. Acad. Sci.*, 2010. **107**, 3293-3298.
41. S. Zhang, M. A. Greenfield, A. Mata, L. C. Palmer, R. Bitton, J. R. Mantei, C. Aparicio, M. O. de la Cruz and S. I. Stupp, *Nat. Mater.*, 2010, **9**, 594-601.
42. E. J. Berns, S. Sur, L. Pan, J. E. Goldberger, S. Suresh, S. Zhang, J. A. Kessler and S. I. Stupp, *Biomaterials*, 2014, **35**, 185-195.
43. V. Jayawarna, M. Ali, T. A. Jowitt, A. F. Miller, A. Saiani, J. E. Gough and R. V. Ulijn, *Adv. Mater.*, 2006, **18**, 611-614.
44. Z. M. Yang, K. M. Xu, Z. F. Guo, Z. H. Guo and B. Xu, *Adv. Mater.*, 2007, **19**, 3152-3156.
45. S. M. Standley, D. J. Toft, H. Cheng, S. Soukasene, J. Chen, S. M. Raja, V. Band, H. Band, V. L. Cryns and S. I. Stupp, *Cancer Research*, 2010, **70**, 3020-3026.

46. Y.-b. Lim, E. Lee and M. Lee, *Angew. Chem. Int. Ed.*, 2007, **46**, 3475-3478.
47. S. Soukasene, D. J. Toft, T. J. Moyer, H. Lu, H.-K. Lee, S. M. Standley, V. L. Cryns and S. I. Stupp, *ACS Nano*, 2011, **5**, 9113-9121.
48. S. Manchineella and T. Govindaraju, *RSC Advances*, 2012, **2**, 5539-5542.
49. N. Wiradharma, Y. W. Tong and Y.-Y. Yang, *Biomaterials*, 2009, **30**, 3100-3109.
50. G. G. Holman, M. Zewail-Foote, A. R. Smith, K. A. Johnson and B. L. Iverson, *Nat. Chem.*, 2011, **3**, 875-881.
51. M. B. Avinash and T. Govindaraju, *Nanoscale*, 2011, **3**, 2536-2543.
52. M. B. Avinash and T. Govindaraju, *Adv. Funct. Mater.*, 2011, **21**, 3875-3882.
53. M. B. Avinash, P. K. Samanta, K. V. Sandeepa, S. K. Pati and T. Govindaraju, *Eur. J. Org. Chem.*, 2013, **2013**, 5838-5847.
54. M. Pandeeswar, M. B. Avinash and T. Govindaraju, *Chem. Eur. J.*, 2012, **18**, 4818-4822.
55. T. Govindaraju, M. Pandeeswar, K. Jayaramulu, G. Jaipuria and H. S. Atreya, *Supramol. Chem.*, 2011, **23**, 487-492.
56. T. Govindaraju, *Supramol. Chem.*, 2011, **23**, 759-767.
57. S. Manchineella, V. Prathyusha, U. D. Priyakumar and T. Govindaraju, *Chem. Eur. J.*, 2013, **19**, 16615-16624.
58. M. B. Avinash and T. Govindaraju, *J. Phys. Chem. Lett.*, 2013, **4**, 583-588.
59. H. Shao, T. Nguyen, N. C. Romano, D. A. Modarelli and J. R. Parquette, *J. Am. Chem. Soc.*, 2009, **131**, 16374-16376.
60. R. Matmour, I. De Cat, S. J. George, W. Adriaens, P. Leclère, P. H. H. Bomans, N. A. J. M. Sommerdijk, J. C. Gielen, P. C. M. Christianen, J. T. Heldens, J. C. M. van Hest, D. W. P. M. Löwik, S. De Feyter, E. W. Meijer and A. P. H. J. Schenning, *J. Am. Chem. Soc.*, 2008, **130**, 14576-14583.
61. S. R. Diegelmann, J. M. Gorham and J. D. Tovar, *J. Am. Chem. Soc.*, 2008, **130**, 13840-13841.
62. H. C. Fry, J. M. Garcia, M. J. Medina, U. M. Ricoy, D. J. Gosztola, M. P. Nikiforov, L. C. Palmer and S. I. Stupp, *J. Am. Chem. Soc.*, 2012, **134**, 14646-14649.
63. M. Reches and E. Gazit, *Science*, 2003, **300**, 625-627.
64. A. Kholkin, N. Amdursky, I. Bdikin, E. Gazit and G. Rosenman, *ACS Nano*, 2010, **4**, 610-614.
65. A. Mahler, M. Reches, M. Rechter, S. Cohen and E. Gazit, *Adv. Mater.*, 2006, **18**, 1365-1370.
66. L. E. R. O'Leary, J. A. Fallas, E. L. Bakota, M. K. Kang and J. D. Hartgerink, *Nat. Chem.*, 2011, **3**, 821-828.
67. J. D. Tovar, B. M. Rabatic and S. I. Stupp, *Small*, 2007, **3**, 2024-2028.
68. A. Herland, P. Björk, K. P. R. Nilsson, J. D. M. Olsson, P. Åsberg, P. Konradsson, P. Hammarström and O. Inganäs, *Adv. Mater.*, 2005, **17**, 1466-1471.
69. Q. Zou, L. Zhang, X. Yan, A. Wang, G. Ma, J. Li, H. Möhwald and S. Mann, *Angew. Chem. Int. Ed.*, 2014, **53**, 2366-2370.
70. M. Endo and H. Sugiyama, *Acc. Chem. Res.*, 2014, **47**, 1645-1653.
71. S. Howorka, *Langmuir*, 2013, **29**, 7344-7353.
72. X. Lan and Q. Wang, *NPG Asia Mater.*, 2014, **6**, e97.
73. S. Modi, M. G. Swetha, D. Goswami, G. D. Gupta, S. Mayor and Y. Krishnan, *Nat. Nanotechnol.*, 2009, **4**, 325-330.
74. S. Surana, J. M. Bhat, S. P. Koushika and Y. Krishnan, *Nat. Commun.*, 2011, **2**, 340.
75. S. Modi, C. Nizak, S. Surana, S. Halder and Y. Krishnan, *Nat. Nanotechnol.*, 2013, **8**, 459-467.
76. A. M. S. Kumar, S. Sivakova, J. D. Fox, J. E. Green, R. E. Marchant and S. J. Rowan, *J. Am. Chem. Soc.*, 2008, **130**, 1466-1476.
77. X. Du, J. Li, Y. Gao, Y. Kuang and B. Xu, *Chem. Commun.*, 2012, **48**, 2098-2100.
78. N. C. Seeman, *Nano Lett.*, 2010, **10**, 1971-1978.
79. A. Kuzuya and M. Komiyama, *Nanoscale*, 2010, **2**, 309-321.
80. S. M. Douglas, I. Bachelet and G. M. Church, *Science*, 2012, **335**, 831-834.
81. Y. Benenson, B. Gil, U. Ben-Dor, R. Adar and E. Shapiro, *Nature*, 2004, **429**, 423-429.
82. J. J. Storhoff and C. A. Mirkin, *Chem. Rev.*, 1999, **99**, 1849-1862.
83. G. P. Spada, S. Lena, S. Masiero, S. Pieraccini, M. Surin and P. Samorì, *Adv. Mater.*, 2008, **20**, 2433-2438.
84. P. G. A. Janssen, J. Vandenbergh, J. L. J. van Dongen, E. W. Meijer and A. P. H. J. Schenning, *J. Am. Chem. Soc.*, 2007, **129**, 6078-6079.
85. R. Iwaura, F. J. M. Hoeben, M. Masuda, A. P. H. J. Schenning, E. W. Meijer and T. Shimizu, *J. Am. Chem. Soc.*, 2006, **128**, 13298-13304.
86. Y. N. Teo and E. T. Kool, *Chem. Rev.*, 2012, **112**, 4221-4245.
87. T. J. Bandy, A. Brewer, J. R. Burns, G. Marth, T. Nguyen and E. Stulz, *Chem. Soc. Rev.*, 2011, **40**, 138-148.
88. Y. Ruff, T. Moyer, C. J. Newcomb, B. Demeler and S. I. Stupp, *J. Am. Chem. Soc.*, 2013, **135**, 6211-6219.
89. N. Narayanaswamy, M. B. Avinash and T. Govindaraju, *New J. Chem.*, 2013, **37**, 1302-1306.
90. P. G. A. Janssen, A. Ruiz-Carretero, D. González-Rodríguez, E. W. Meijer and A. P. H. J. Schenning, *Angew. Chem. Int. Ed.*, 2009, **48**, 8103-8106.
91. A. Ruiz-Carretero, P. G. A. Janssen, A. L. Stevens, M. Surin, L. M. Herz and A. P. H. J. Schenning, *Chem. Commun.*, 2011, **47**, 884-886.
92. T. Nguyen, A. Brewer and E. Stulz, *Angew. Chem. Int. Ed.*, 2009, **48**, 1974-1977.
93. F. Garo and R. Häner, *Angew. Chem. Int. Ed.*, 2012, **51**, 916-919.
94. C. Wang, Z. Huang, Y. Lin, J. Ren and X. Qu, *Adv. Mater.*, 2010, **22**, 2792-2798.
95. S. Venkataraman, R. M. Dirks, P. W. K. Rothemund, E. Winfree and N. A. Pierce, *Nat. Nanotechnol.*, 2007, **2**, 490-494.
96. Z.-G. Wang, J. Elbaz and I. Willner, *Nano Lett.*, 2010, **11**, 304-309.
97. P. H. Seeberger, *Nat. Chem. Biol.*, 2009, **5**, 368-372.
98. K. R. Love and P. H. Seeberger, *Angew. Chem. Int. Ed.*, 2002, **41**, 3583-3586.
99. M. Sánchez-Navarro, A. Muñoz, B. M. Illescas, J. Rojo and N. Martín, *Chem. Eur. J.*, 2011, **17**, 766-769.
100. J. Luczkowiak, S. Sattin, I. Sutkevičiūtė, J. J. Reina, M. Sánchez-Navarro, M. Thépaut, L. Martínez-Prats, A. Daghetti, F. Fieschi, R. Delgado, A. Bernardi and J. Rojo, *Bioconjugate Chem.*, 2011, **22**, 1354-1365.
101. A. V. Pukin, H. M. Branderhorst, C. Sisu, C. A. G. M. Weijers, M. Gilbert, R. M. J. Liskamp, G. M. Visser, H. Zuilhof and R. J. Pieters, *ChemBioChem*, 2007, **8**, 1500-1503.
102. C. Sisu, A. J. Baron, H. M. Branderhorst, S. D. Connell, C. A. G. M. Weijers, R. de Vries, E. D. Hayes, A. V. Pukin, M. Gilbert, R. J.

Pieters, H. Zuilhof, G. M. Visser and W. B. Turnbull, *ChemBioChem*, 2009, **10**, 329-337.
103. M. Durka, K. Buffet, J. Iehl, M. Holler, J.-F. Nierengarten, J. Taganna, J. Bouckaert and S. P. Vincent, *Chem. Commun.*, 2011, **47**, 1321-1323.
104. R. U. Kadam, M. Bergmann, M. Hurley, D. Garg, M. Cacciarini, M. A. Swiderska, C. Nativi, M. Sattler, A. R. Smyth, P. Williams, M. Cámara, A. Stocker, T. Darbre and J.-L. Reymond, *Angew. Chem. Int. Ed.*, 2011, **50**, 10631-10635.
105. E. L. Dane, A. E. Ballok, G. A. O'Toole and M. W. Grinstaff, *Chem. Sci.*, 2014, **5**, 551-557.
106. S. Cecioni, R. Lalor, B. Blanchard, J.-P. Praly, A. Imberty, S. E. Matthews and S. Vidal, *Chem. Eur. J.*, 2009, **15**, 13232-13240.
107. M. C. Hewitt, D. A. Snyder and P. H. Seeberger, *J. Am. Chem. Soc.*, 2002, **124**, 13434-13436.
108. P. H. Seeberger, R. L. Soucy, Y.-U. Kwon, D. A. Snyder and T. Kanemitsu, *Chem. Commun.*, 2004, 1706-1707.
109. I. J. Krauss, J. G. Joyce, A. C. Finnefrock, H. C. Song, V. Y. Dudkin, X. Geng, J. D. Warren, M. Chastain, J. W. Shiver and S. J. Danishefsky, *J. Am. Chem. Soc.*, 2007, **129**, 11042-11044.
110. S. Dziadek, A. Hobel, E. Schmitt and H. Kunz, *Angew. Chem. Int. Ed.*, 2005, **44**, 7630-7635.
111. D. Grünstein, M. Maglinao, R. Kikkeri, M. Collot, K. Barylyuk, B. Lepenies, F. Kamena, R. Zenobi and P. H. Seeberger, *J. Am. Chem. Soc.*, 2011, **133**, 13957-13966.
112. K. Gruber, T. Horlacher, R. Castelli, A. Mader, P. H. Seeberger and B. A. Hermann, *ACS Nano*, 2011, **5**, 3670-3678.
113. A. Mader, K. Gruber, R. Castelli, B. A. Hermann, P. H. Seeberger, J. O. Rädler and M. Leisner, *Nano Lett.*, 2011, **12**, 420-423.
114. K.-R. Wang, H.-W. An, Y.-Q. Wang, J.-C. Zhang and X.-L. Li, *Org. Biomol. Chem.*, 2013, **11**, 1007-1012.
115. V. Dhaware, A. Y. Shaikh, M. Kar, S. Hotha and S. Sen Gupta, *Langmuir*, 2013, **29**, 5659-5667.
116. K. Petkau-Milroy and L. Brunsveld, *Eur. J. Org. Chem.*, 2013, **2013**, 3470-3476.
117. O.-K. Kim, J. Melinger, S.-J. Chung and M. Pepitone, *Org. Lett.*, 2008, **10**, 1625-1628.
118. D. Wu, J. Zhou, J. Shi, X. Du and B. Xu, *Chem. Commun.*, 2014, **50**, 1992-1994.
119. X. Li, X. Du, Y. Gao, J. Shi, Y. Kuang and B. Xu, *Soft Matter*, 2012, **8**, 7402-7407.
120. L. S. Birchall, S. Roy, V. Jayawarna, M. Hughes, E. Irvine, G. T. Okorogheye, N. Saudi, E. De Santis, T. Tuttle, A. A. Edwards and R. V. Ulijn, *Chem. Sci.*, 2011, **2**, 1349-1355.
121. Y. Ogawa, C. Yoshiyama and T. Kitaoka, *Langmuir*, 2012, **28**, 4404-4412.
122. A. Vidyasagar, K. Handore and K. M. Sureshan, *Angew. Chem. Int. Ed.*, 2011, **50**, 8021-8024.
123. L. Zhang, J. M. Chan, F. X. Gu, J.-W. Rhee, A. Z. Wang, A. F. Radovic-Moreno, F. Alexis, R. Langer and O. C. Farokhzad, *ACS Nano*, 2008, **2**, 1696-1702.
124. J. M. Chan, J.-W. Rhee, C. L. Drum, R. T. Bronson, G. Golomb, R. Langer and O. C. Farokhzad, *Proc. Natl. Acad. Sci.*, 2011, **108**, 19347-19352.
125. Y. Dong, K. T. Love, J. R. Dorkin, S. Sirirungruang, Y. Zhang, D. Chen, R. L. Bogorad, H. Yin, Y. Chen, A. J. Vegas, C. A. Alabi, G. Sahay, K. T. Olejnik, W. Wang, A. Schroeder, A. K. R. Lytton-Jean, D. J. Siegwart, A. Akinc, C. Barnes, S. A. Barros, M. Carioto, K. Fitzgerald, J. Hettinger, V. Kumar, T. I. Novobrantseva, J. Qin, W. Querbes, V. Koteliansky, R. Langer and D. G. Anderson, *Proc. Natl. Acad. Sci.*, 2014, **111**, 3955-3960.
126. J. J. Hwang, S. N. Iyer, L.-S. Li, R. Claussen, D. A. Harrington and S. I. Stupp, *Proc. Natl. Acad. Sci.*, 2002, **99**, 9662-9667.
127. Y. Fujimoto, K. Mitsunobe, S. Fujiwara, M. Mori, M. Hashimoto, Y. Suda, S. Kusumoto and K. Fukase, *Org. Biomol. Chem.*, 2013, **11**, 5034-5041.
128. Y. Yang, S. Oishi, C. E. Martin and P. H. Seeberger, *J. Am. Chem. Soc.*, 2013, **135**, 6262-6271.
129. E. Schaeffer, L. Dehuyser, D. Sigwalt, V. Flacher, S. Bernacchi, O. Chaloin, J.-S. Remy, C. G. Mueller, R. Baati and A. Wagner, *Bioconjugate Chem.*, 2013, **24**, 1813-1823.
130. D. Asthana, A. Kumar, A. Pathak, P. K. Sukul, S. Malik, R. Chatterjee, S. Patnaik, K. Rissanen and P. Mukhopadhyay, *Chem. Commun.*, 2011, **47**, 8928-8930.
131. B. K. Ng, T. S. Velayutham, W. C. Gan, W. H. A. Majid, V. Periasamy, R. Hashim and N. I. M. Zahid, *Ferroelectrics*, 2013, **445**, 67-73.
132. C. Ingrosso, G. V. Bianco, M. Corricelli, A. Corcelli, S. Lobasso, G. Bruno, A. Agostiano, M. Striccoli and M. L. Curri, *Chem. Commun.*, 2013, **49**, 6941-6943.
133. M. Assali, J.-J. Cid, I. Fernández and N. Khiar, *Chem. Mater.*, 2013, **25**, 4250-4261.
134. M. J. Clemente, J. Fitremann, M. Mauzac, J. L. Serrano and L. Oriol, *Langmuir*, 2011, **27**, 15236-15247.
135. R. Ochi, K. Kurotani, M. Ikeda, S. Kiyonaka and I. Hamachi, *Chem. Commun.*, 2013, **49**, 2115-2117.
136. A. Ajayaghosh, C. Vijayakumar, R. Varghese and S. J. George, *Angew. Chem. Int. Ed.*, 2006, **45**, 456-460.